Redactie

ON THE FILM AND THE FOUNTAIN EFFECT IN HELIUM II

C. J. N. VAN DEN MEIJDENBERG

ON THE FILM AND THE FOUNTAIN EFFECT IN HELIUM II

ON THE FILM AND THE FOUNTAIN EFFECT IN HELIUM II

PROEFSCHRIFT

TER VERKRIJGING VAN DE GRAAD VAN DOCTOR IN DE WIS- EN NATUURKUNDE AAN DE RIJKSUNIVERSITEIT TE LEIDEN, OP GEZAG VAN DE RECTOR MAGNIFICUS MR J. V. RIJPPERDA WIERDSMA, HOOGLERAAR IN DE FACULTEIT DER RECHTSGELEERDHEID, TEGEN DE BEDENKINGEN VAN DE FACULTEIT DER WIS- EN NATUURKUNDE TE VERDEDIGEN OP WOENSDAG 12 APRIL 1961 TE 16 UUR

DOOR

CORNELIS JOHANNES NICOLAAS VAN DEN MEIJDENBERG

GEBOREN TE WAALWIJK IN 1929

Promotor: PROF. DR K. W. TACONIS

AAN DE NAGEDACHTENIS VAN MIJN VADER
AAN MIJN MOEDER
AAN MIJN VROUW

STELLINGEN

I

De waarden voor de parameters van het excitatiespectrum van Helium II afgeleid uit metingen van neutronenverstrooiing, komen niet overeen met de waarden die gevonden worden uit de experimentele gegevens van de soortelijke warmte en de voortplantingssnelheid van "second sound". Deze discrepantie is toe te schrijven aan het verschil tussen het werkelijke excitatiespectrum en de door Landau ingevoerde benadering van het spectrum.

L. D. Landau, J. Phys. U.S.S.R. **11** (1947) 91.
Dit proefschrift, Hoofdstuk I, 5.

II

Rohrschach en Romberg besluiten uit hun experimenten over de drukgradient veroorzaakt door een warmtestroom in Helium II, dat het niet mogelijk is met het twee-fluida-model de door hen waargenomen verschijnselen te verklaren. Deze conclusie is niet gerechtvaardigd.

H. E. Rohrschach en F. A. Romberg, Proc. Vth Int. Conf. on Low Temp. Phys. Madison U.S.A. (1957) p. 35.

III

De bereiding van HD door omzetting van H_2 en D_2 tot de evenwichtssamenstelling en scheiding van het zo verkregen mengsel door rectificatie biedt vele voordelen boven de gebruikelijke chemische bereidingswijze.

IV

Het is gewenst de afhankelijkheid van de dampspanning van vloeibaar ^{3}He van de temperatuur rechtstreeks met de gasthermometer te bepalen. Dit geldt vooral voor het temperatuurgebied tussen 1 en 2 °K.

V

De in het Duitse ontwerp-normaalblad "Torsionsschwingungsversuch" gegeven formule voor de glijdingsmodulus G is onjuist.

Prüfung von Kunststoffen, Torsionsschwingungsversuch, Entwurf DIN 53445 (1958).

VI

Bij experimenten over de voortplanting van warmtepulsen in Helium II bij lage temperatuur is het gewenst dat de apparatuur de ontvangen pulsen onvervormd weergeeft.

H. C. Kramers, Proefschrift Leiden 1956.
D. J. Sandiford en H. A. Fairbank, Programme VIIth Int. Conf. on Low Temp. Phys. Toronto, Canada. (1960) p. 404.

VII

Een verfijning van de metingen van Dash *e.a.*, betreffende het Mösbauer-effect van ^{57}Fe bij zeer lage temperaturen, zou van belang zijn voor de studie van zowel de invloed van K-vangst op de kernspinrichting als de hyperfijn-structuursplitsingen.

J. G. Dash, R. D. Taylor, P. P. Craig, D. E. Nagle, D. R. F. Cochran en W. E. Keller, Phys. Rev. Letters **5** (1960) 152.

VIII

Goldstein heeft gewezen op de mogelijkheid van het optreden van een minimum in de smeltkromme van ^4He. Op grond van de thans beschikbare gegevens kan worden verwacht dat het maximale verschil tussen de minimum smeltdruk en de smeltdruk bij 0 °K niet meer bedraagt dan 0.04 atm, terwijl de temperatuur waarbij het minimum eventueel optreedt lager is dan 0.8 °K.

IX

De interpretatie die Kidder en Fairbank geven aan de resultaten van hun onderzoek naar de stromingseigenschappen van superfluide helium in een wijde capillair is onjuist.

J. N. Kidder en W. M. Fairbank, Programme VIIth Int. Conf. on Low Temp. Phys. Toronto, Canada. (1960) p. 92.

X

Het verdient aanbeveling dat in fysische leerboeken de zogenaamde deltafunctie op wiskundig juiste wijze wordt ingevoerd en behandeld.

P. M. Morse en H. Feshbach, Methods of Theoretical Physics, I, McGraw Hill (1953) p. 122, 123.

XI

Tegen de wijze waarop het examen voor de natuurkunde bij het middelbaar onderwijs geregeld is zijn ernstige bezwaren aan te voeren.

Na beëindiging van mijn middelbare schoolopleiding aan de R.K. H.B.S. (thans Dr Mollercollege) te Waalwijk begon ik in 1946 mijn studie in de wis- en natuurkunde aan de Universiteit te Leiden. In 1950 legde ik het candidaatsexamen A af en in juni 1953 volgde het doctoraal examen experimentele natuurkunde met als bijvak wiskunde.

Mijn werkzaamheden op het Kamerlingh Onnes Laboratorium vingen aan in september 1950. Gedurende de eerste jaren assisteerde ik achtereenvolgens: P. Dekking bij een onderzoek over het fase-evenwicht van edelgassen, Dr H. H. Tjerkstra bij metingen over adsorptie van helium en Prof. Dr J. G. Aston (Pennsylvania State University, Pennsylvania, U.S.A.) bij onderzoekingen betreffende de transportsnelheid en de snelheid van second sound in de helium film. Als medewerker van de heliumwerkgroep onder leiding van Prof. Dr K. W. Taconis verrichtte ik in 1953, in samenwerking met Dr J. J. M. Beenakker en Dr D. H. N. Wansink, een onderzoek over het fonteineffect in ^{4}He.

Van april 1954 tot januari 1956 moest ik mijn werkzaamheden op het Kamerlingh Onnes Laboratorium onderbreken voor het vervullen van mijn militaire dienstplicht. Gedurende de militaire dienst werd ik opgeleid tot officier der verbindingsdienst.

Begin 1956 keerde ik terug in de helium-werkgroep en vanaf maart 1956 hield ik mij bezig met de onderzoekingen die in dit proefschrift beschreven zijn. Bij de experimenten, welke medio 1959 werden afgesloten, werd ik terzijde gestaan door R. de Bruyn Ouboter en C. le Pair. Bij het daarna verrichte theoretische onderzoek gaf Prof. Dr H. Matsuda (Kyoto University, Kyoto, Japan) vele waardevolle adviezen. In 1960 maakte ik gedurende korte tijd een studiereis door de Verenigde Staten van Amerika en Canada.

Inmiddels gaf ik vanaf 1956 leiding aan het natuurkundig practicum voor medische studenten, terwijl ik vanaf november 1956 tevens de functie vervulde van leraar aan het Gemeentelijk Instituut voor middelbare akten in de exacte vakken te 's-Gravenhage. In 1958 werd ik benoemd tot wetenschappelijk ambtenaar.

CONTENTS

INTRODUCTION AND REVIEW OF THE EXPERIMENTS PERFORMED

The investigations which are the subject of this thesis deal mainly with two phenomena proper to Helium II, *viz.* the fountain effect and the creeping helium film. These two at first sight little allied studies, originated from an early experiment[1]) concerned with both phenomena. In the experiment in question the fountain effect in Helium II was indirectly investigated by measuring the pressure of the helium gas in equilibrium with the film when a fountain pressure was exerted upon the film. This experiment gave rise, on one hand, to a further investigation of the fountain effect, and on the other to a study of the influence of large pressure heads on the flow properties of the film. It seems therefore useful to start here with a brief review of the early indirect measurements of the fountain effect.

If of two vessels A and B connected by a superleak (see fig. 1), the lower cold one, A, contains some Helium II, a small temperature difference between A and B is sufficient to transfer all the liquid by film creep to the higher, warm vessel, B. If still larger temperature differences are created, it is observed that the pressure in the cold vessel becomes lower than the saturated vapour pressure corresponding to the temperature T_A of the vessel. This results from the fact that the helium film remaining in A has become unsaturated under the influence of the fountain force acting indirectly on the superfluid in the film. The decrease of the pressure below the saturated vapour pressure, Δp_A, is related to the temperature difference, ΔT, from which this pressure decrease originates.

To establish the relation between Δp_A and ΔT we first consider a high vessel which contains some Helium II and which is completely surrounded by a helium bath at constant temperature. The film covering the entire wall of the vessel is, at any height h, in equilibrium with the gas. The chemical potential of the film, μ_f, is then equal to the chemical potential of the gas, μ_g, but is a function of h, for the pressure of the gas decreases with increasing height. Considering the change in the chemical potential of the film with height and comparing it with the corresponding change in the chemical potential of the gas we find

$$d\mu_f = d\mu_g$$

However, since the temperature is the same throughout the vessel we can write

$$(\partial \mu_f/\partial p)\, \mathrm{d}p_f = (\partial \mu_g/\partial p)\, \mathrm{d}p_g$$

or

$$v_f\, \mathrm{d}p_f = v_g\, \mathrm{d}p_g$$

where v_f and v_g are the specific volumes of film and gas respectively. Introducing densities we obtain

$$\mathrm{d}p_g = (\rho_g/\rho_f)\, \mathrm{d}p_f \tag{1}$$

As the pressure of the gas is almost the saturated vapour pressure, the thickness of the film is of the order of ten statistical layers or more. The surface layers of the film which is in equilibrium with the gas, have a density practically equal to the density of bulk liquid, ρ_l. By substitution in (1) we get

$$\mathrm{d}p_g = (\rho_g/\rho_l)\, \mathrm{d}p_f \tag{2}$$

Integration of (2) yields

$$\Delta p_g = (\bar{\rho}_g/\rho_l)\, \Delta p_f \tag{3}$$

where Δp_g denotes the difference between the pressure of the gas at a height h and the saturated vapour pressure ($\Delta p_g = h\bar{\rho}_g$), Δp_f the corresponding pressure decrease in the film ($\Delta p_f = h\rho_l$) and $\bar{\rho}_g$ the mean density of the gas in the range of the pressure variation Δp_g.

Let us now consider the situation in vessel A of the apparatus shown in fig. 1. The only difference from the preceding case is that here Δp_f is created by means of a temperature difference between A and B. Thus Δp_f is now a fountain pressure for which we can write

$$\Delta p_f = \int_{T_A}^{T_B} f\, \mathrm{d}T$$

where f is the fountain height per unit temperature difference. Substitution of this expression in (3) finally gives

$$\Delta p_g = (\bar{\rho}_g/\rho_l) \int_{T_A}^{T_B} f\, \mathrm{d}T. \tag{4}$$

According to eq. (4) the fountain height $\int f\, \mathrm{d}T$ can be determined by measuring Δp_g, *i.e.* the pressure decrease of the gas. We point here to a principal difference between this method and the direct measurement of the fountain effect. The height difference per millidegree temperature difference between the liquid levels of the Helium II in the two vessels connected by a narrow capillary, increases with temperature and becomes very large near the λ-temperature. For this reason only small temperature differences can be used and the accuracy depends on the measurement of ΔT.

The indirect method, on the other hand, is especially accurate for large temperature differences corresponding to fountain heights of some meters helium, since the pressure difference which is to be measured here is a factor ρ_g/ρ_l smaller than in the direct method.

The experiment was performed with the apparatus shown in fig. 1. The

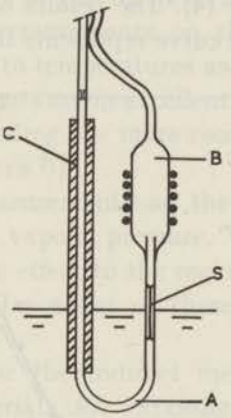

Fig. 1. Apparatus.

reservoir B and the copper capillary A are connected through a superleak S. From A and B german silver capillaries lead to outside the cryostat where they are connected with an oil manometer. The connecting capillaries can move through the top of the cryostat so that it is possible to adjust the height of the apparatus in the surrounding helium bath. In vessel A the heat leak is mainly caused by the film creeping in the capillary leading to the top of the cryostat and it is considerably reduced by the narrow constriction mounted in the capillary. In addition the capillary is surrounded with a cotton wick C up to a few cm below the constriction. In this way temperature effects as a result of the lowering of the bath level were negligible. The slight heat contact between the capillaries above the reservoir B proved to be necessary to obtain a stable adjustment of the temperature during the heating of B. During the measurements the height of the apparatus was always adjusted so that the bath level was half way to the superleak. On the oil manometer the pressure difference Δp_A between bath and vessel A was determined as a function of the temperature difference ΔT between bath and vessel B at bath temperatures varying between 1.45 and 2.15°K. For temperatures near the λ-point it was desirable to use a superleak of high capacity because of the low transfer rates, especially by unsaturated films. We used a jewellers rouge leak for the measurements at higher temperatures; it was nevertheless difficult to reach equilibrium above 2.0°K. For the measurements at the lowest temperatures a platinum-in-pyrex glass superleak was used.

We calculated the integrated fountain height by using H. London's

formula, $\int f \, dT = \rho_1 \int S_1 \, dT$ with the entropy values as derived from specific heat measurements by Kramers, Wasscher and Gorter [2]). The graph Δp_A *versus* the integrated fountain height showed straight lines going through the origin. (The pressure variation of ρ_g was, at most, a few per cent). From the slopes of these lines the density of the gas in A could be derived according to eq. (4). The results of this calculation are shown plotted in fig. 2. The dashed curve represents the density as calculated from

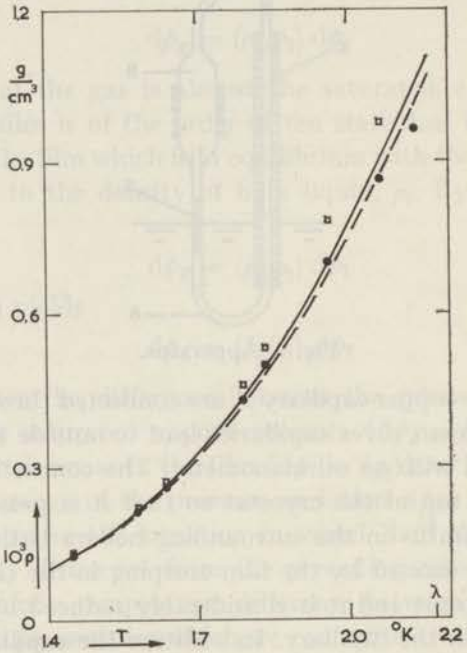

Fig. 2. Correspondence between the gas densities derived from eq. (4) (points) and the calculated gas densities (curves).
Dashed curve: calculated from ideal gas law
Solid curve : calculated with B-values.
●: f from entropy data of Kramers *e.a.*
□: f from the data of Meyer and Mellink [4]).

the ideal gas law and the solid curve gives this density corrected with the B-values measured by Kistemaker [3]). The points indicate the densities obtained from the aforementioned calculation. Apart from the deviations above 2.0°K, which could be explained on the basis of non-equilibrium states, the densities were found to be in agreement with the corrected densities (solid curve) within the limits of accuracy. We could therefore conclude that the fountain heights were in agreement with H. London's formula.

When, however, the integrated fountain height was calculated using for f the smoothed values derived from the in 1954 existing direct measure-

ments of the fountain effect [4]), less good agreement was found. In this case deviations up to 10% from the corrected densities appeared.

Since we performed this experiment H. London's formulae for the fountain effect and the mechanocaloric effect have been verified in a wide temperature region by various authors. We may mention *e.g.* the measurements on the fountain effect in the temperature region from 0.82–1.59°K by Peshkov [5]) and the measurements on the fountain effect and the mechanocaloric effect down to temperatures as low as 0.2°K by Bots and Gorter [6]). These measurements are in excellent agreement with the entropy data of Kramers *e.a.* (Including the more recent data of Wiebes, Niels-Hakkenberg and Kramers [7])).

Up to this point the measurements on the fountain effect dealt with Helium II at the saturated vapour pressure. We have now extended the investigation on the fountain effect to the region of Helium II at moderate pressures above 1°K. A full account of these measurements is given in chapter I.

The method employed for the indirect measurement of the fountain effect proved to be appropriate for exposing the film to a welldefined pressure head. Many experiments on the flow properties of the film had been made but in most experiments the driving force acting on the film originated from a relatively small hydrostatic pressure head. Using our method it appeared possible to investigate the flow properties of the film at large pressure heads and to obtain in this way an answer to the question of whether indeed a dependence of the flow rate on pressure head exists. Moreover, the method seemed to be especially suitable for measuring the flow rate of the film in equilibrium with mixtures of ^{3}He and ^{4}He. Since in this case, however, the osmotic pressure of the mixture in the lower vessel acts opposite to the pressure head across the superleak it was more practical to exert a tension on the film by means of a mixture of higher concentration in the upper vessel. In Chapter II such measurements on the film flow rate of mixtures are described.

In order to understand the behaviour of the creeping film the properties of the static helium film should be known. The zero point energy of the atoms in the film is found to play a dominant role in the problem of the static helium film. However, up to now, a satisfactory quantitative approach has not been achieved. Some theoretical considerations connected with this problem are given in chapter III.

REFERENCES

1) Van den Meijdenberg, C. J. N., Taconis, K. W., Beenakker, J. J. M. and Wansink, D. H. N., Commun. Kamerlingh Onnes Lab., Leiden No. 295*c*; Physica **20** (1954) 157.

2) Kramers, H. C., Wasscher, J. D. and Gorter, C. J., Commun. No. 288*c*; Physica **18** (1952) 329.

3) Kistemaker, J., Commun. No. 269*b*; Physica **12** (1946) 227.

4) Kapitza, P. L., J. Phys. U.S.S.R. **5** (1941) 59.
Meyer, L. and Mellink, J. H., Commun. No. 272*b*; Physica **13** (1947) 197.
5) Peshkov, V. P., Zh. eksper. teor. Fiz. U.S.S.R. **29** (1954) 351.
6) Bots, G. J. C. and Gorter, C. J., Commun. No. 304*b*; Physica **22** (1956) 503;
Bots, G. J. C. and Gorter, C. J., Commun. No. 320*a*; Physica **26** (1960) 337.
Bots, G. J. C., Thesis Leiden 1959.
7) Wiebes, J., Niels-Hakkenberg, C. G. and Kramers, H. C. Commun. No. 308*a*; Physica **23** (1957) 625.

CHAPTER I

THE ENTROPY OF HELIUM II UNDER PRESSURE FROM MEASUREMENTS ON THE FOUNTAIN EFFECT

Synopsis

Assuming that London's formula, $\Delta p = \varrho S \Delta T$, is also valid for the fountain effect in Helium II at high pressures, the entropy as a function of temperature and pressure has been evaluated from measurements of the fountain effect in the temperature range 1.15–2.00°K and at various pressures between the saturated vapour pressure and 25 atm. On extrapolating the entropy data as a function of pressure to the saturated vapour pressure good agreement has been found with the entropy values of Kramers *e.a.*., the deviations being smaller than 2%. The entropy data of Lounasma and Kojo at different densities have been fitted to the present entropy data to obtain an entropy diagram up to the λ-curve. As, however, the various data on the density of liquid helium do not agree there is some doubt with respect to this fit.

Finally, values have been determined for the parameters of the roton spectrum at several pressures. The results have been discussed and compared with those obtained from experiments on inelastic neutron scattering.

1. *Introduction.* From various experiments [1]) on the fountain effect in Helium II at the saturated vapour pressure it has been found that the fountain pressure Δp originating from a temperature difference ΔT across a narrow channel is in agreement with the formula of H. London

$$\Delta p = \rho S \Delta T \tag{1}$$

within the limits of experimental accuracy; ρ is the density of the liquid and S the entropy per unit mass. This agreement is a justification of the special approach of London [2]) and later of Landau [2]) in deriving formula (1) on the basis of the two fluid model by assuming the entropy of the superfluid to be zero, or at least negligibly small compared to the total entropy of the liquid. If it is assumed that London's formula is valid in the entire Helium II region, which is plausible indeed, the entropy of the helium liquid under pressure may be determined by measurements of the fountain pressure.

The appropriate apparatus for measurements of the fountain effect consists of two vessels connected by a superleak, and the experiment is

simply based on the measurements of the pressure difference as a function of the temperature difference imposed across the superleak, under various conditions with respect to temperature and external pressure of the Helium II in the apparatus. In experiments on the fountain effect at the saturated vapour pressure the fountain pressure can be determined from the hydrostatic pressure of the liquid helium. As was pointed out to us by Dr. J. J. M. Beenakker the fountain pressure also can be measured at high pressures by balancing it with a gas pressure difference instead of a hydrostatic pressure head.

2. *Method and apparatus.* Fig. 1 shows a schematic diagram of the apparatus. S is the superleak across which a temperature difference can be established by means of the heater H, while the temperature rise can be measured at the copper block B; S, H and B are inside a vacuum jacket

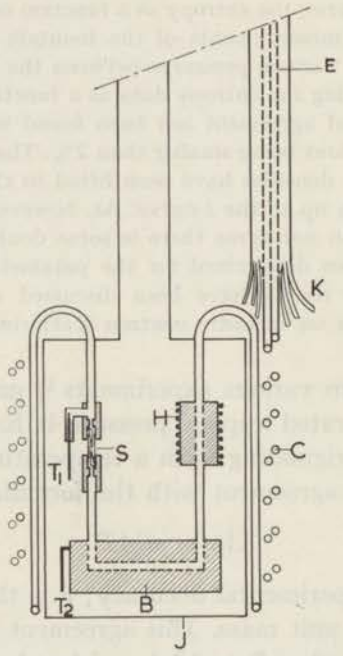

Fig. 1. Apparatus.

J. Superleak and heater are connected with the copper block by stainless steel capillaries of 1 mm inside diameter. From the upper ends of S and H similar stainless steel capillaries lead outside the vacuum jacket where they are connected to spirally wound copper capillaries of 1 m length and 1 mm inside diameter. Finally, stainless steel capillaries E lead to the top of the cryostat and outside the cryostat to a differential oil manometer

of thick walled glass, so as to stand pressures up to 30 atm. The fountain pressure can be measured on this oil manometer *).

The method in determining the fountain pressure from the oil manometer readings outside the cryostat may be explained here more extensively. The true pressure difference across the superleak is observed on the oil manometer only if the pressure gradients in the helium inside the capillaries leading to the manometer are equal. Primarily the pressure gradients are due to the weight of the helium columns but moreover, as a consequence of the special mechanism of the heat conduction in Helium II, a pressure gradient may also arise from the heat flow in the capillaries. Actually, heat is supplied by the heater H and there is also a heat flow coming down through the capillaries E due to the heat leak from the top of the cryostat. If we first consider the situation with respect to the pressure gradients in the capillaries E, neglecting for the moment the influence of the heat flow from the heater, we may state from considerations of symmetry that the true pressure difference is given by the oil manometer if the temperature gradients in the capillaries E are equal. For this reason the capillaries E have been soldered to each other throughout their length and the thermal contact has further been improved by a number of copper strips of about 1 cm length connecting both capillaries. Moreover, up to $\frac{3}{4}$ of their height, the capillaries E have been surrounded by some cotton cords K, covered with a piece of oiled cloth.

The copper strips also increase the heat leak from the top of the cryostat considerably. However, this heat current should flow off to the bath completely so that the temperature at the upper end of the superleak is that of the bath. This has been realized by mounting two long copper capillaries C outside the vacuum jacket. The large surface of the tubes strongly reduces the Kapitza boundary resistance between the helium inside and outside the capillaries. If, as a result of these measures, the oil manometer shows no pressure difference when no heat is supplied by H, this indicates already that the aforementioned experimental conditions are satisfied. A pressure difference zero on the oil manometer, when no heat is supplied, implies that there is no temperature difference or pressure difference across the superleak.

We may now examine the influence of the heat flow from the heater on the pressure gradient. By calculating approximately the temperature gradient in capillary C due to the heat flow from the heater, using the existing data on the Kapitza resistance [3]) and the heat conductivity [4]) of Helium II at the saturated vapour pressure, it is found that at the lowest bath temperature, for example, a temperature difference of 80 millidegrees

*) Relatively speaking, the fountain pressure is measured more sensitively from the hydrostatic pressure of liquid helium due to its low density. Evidently, this method can not be applied in experiments at high pressure.

between the liquid inside and outside the capillary reduces to 1 millidegree within a length of about 20 cm. Although at higher temperatures the heat conductivity is larger, the temperature difference of 1 millidegree is attained within the same or even a shorter length here because the Kapitza resistance and the temperature differences employed are smaller. Hence, the capillary appears to be always sufficiently long to dissipate the heat flow from the heater.

The temperature gradient in capillary C due to the heat current also gives rise to a density gradient in the liquid. As, however, the effective height of the spirally wound capillary is relatively small and moreover as $(\partial\rho/\partial T)_P$ is small [5]) in the Helium II region, the maximum contribution to the pressure difference is smaller than some 10^{-2} mm oil.

If, furthermore, the fountain pressure corresponding to a Poiseuille flow of the normal fluid in the copper capillary is calculated, using the data on the normal fluid viscosity of Brewer and Edwards [6]), its maximum value is found to be also smaller than some 10^{-2} mm oil. From this calculation we concluded in the beginning that the correction on the observed pressure difference due to the fountain pressure in the wide capillary should be negligibly small. Afterwards this conclusion appeared to be premature because in the calculation we wrongly disregarded the fact that the normal fluid flow might be turbulent, and a turbulent flow, indeed, may give rise to a larger pressure gradient. This will be discussed in more detail, however, in the next section, when we deal with the results of the measurements.

Finally we may note that the fountain pressure across the superleak is generally small compared to the pressure in the apparatus. The density difference corresponding to the pressure difference in the capillaries E is, in any case, negligibly small.

The fountain pressure Δp is now equal to the pressure difference in the oil manometer, and is given by $\Delta p = h(\rho_{\text{oil}} - \rho_{\text{gas}})$ if h is the difference in height of the oil levels and ρ_{oil} and ρ_{gas} the density of the oil and the helium gas in the manometer respectively. It is only at high pressures that the density of the helium gas is of some importance; at 30 atm $\rho_{\text{gas}}/\rho_{\text{oil}} \approx$ $\approx 6 \times 10^{-3}$. The influence of the pressure on the density of the oil (octoil S), however, has experimentally been found to be negligibly small in the pressure range considered.

The superleak consists of jewellers rouge, tightly compressed into a stainless steel tube of about 2 cm length and 1.5 mm inside diameter. In order to keep the powder together, on both sides a needle has been pressed into it. The needles are fixed by small brass caps, which are connected to the ends of the stainless steel tube (fig. 1). This type of superleak has been found to stand the repeated warming up and cooling down between many experiments without changing its porosity.

The temperatures are measured by means of the De Vroomen type carbon

resistance thermometers T_1 and T_2 which are included in a double Wheatstone bridge. This bridge consists of three parallel-wired branches of which two branches contain a thermometer in series with a variable resistance and the third branch contains two constant serial resistances. The thermometer branch of T_1 and the branch of constant resistances can be combined in a Wheatstone bridge to measure the bath temperature; by combining the two thermometer branches in a Wheatstone bridge the temperature difference is measured nearly independent of the variations of the bath temperature. The copper body of thermometer T_1 has been brought into direct contact with the helium inside the capillary at the upper end of the superleak in order to avoid influencing the temperature indication by the very small heat flow leaking through the metal wall of the superleak. Thermometer T_2 has been mounted on the copper block B. As the heat leak through the superleak is very small, no temperature gradient exists in the liquid between the heater and the superleak and T_2 therefore indicates the temperature at the lower end of the superleak.

The apparatus is filled with helium from a high pressure helium gas cylinder and the pressure in the apparatus is contineously measured on accurately calibrated Bourdon gauges, one for the pressure range of 0–5 atm, with an accuracy of 0.005 atm, the other for the range of 5–30 atm with an accuracy of 0.01 atm.

For the measurements at one definite bath temperature the thermometer T_2 was calibrated against bath pressure with zero heater current in a range of about 0.3°K in the vicinity of the bath temperature in question, in steps of 0.05°K or smaller. When the values of $(1/R)(\mathrm{d}R/\mathrm{d}T)$ derived from the calibration curves of different days were plotted on one graph, the separate curves were found to lie on one curve within an accuracy of 2%. Small deviations near the ends of the separate curves were corrected by means of this graph. During the experiment the thermometer T_1, and thus the bath temperature, was kept constant within about 10^{-4}°K by monitoring the bath pressure, and the fountain pressure Δp was then measured as a function of the temperature difference ΔT at different pressures P. During a series of measurements of Δp *versus* ΔT a small change of the pressure P, due to the change of the bath level, was generally observed. After all the measurements had been performed the separate values of Δp could be corrected for the difference between the actual pressure at the moment of observation and the mean pressure during the whole series. As the maximum pressure variation is about 0.1 atm, these corrections are negligibly small for almost all measurements.

The relation between Δp and ΔT in first approximation is found to be linear. At large temperature differences, however, deviations from the linear relation appear, as may be explained from the strong dependence of entropy on temperature below the λ-temperature. Assuming the density

to be constant in the range of temperature variation ΔT we may write:

$$\Delta p = \int_{T_0}^{T_0+\Delta T} \rho S \, dT = \rho S_0 \Delta T + \tfrac{1}{2}\rho \left(\frac{\partial S}{\partial T}\right)_0 (\Delta T)^2 + \tfrac{1}{6}\rho \left(\frac{\partial^2 S}{\partial T^2}\right)_0 (\Delta T)^3 + \ldots \quad (2)$$

where the quantities labelled with the suffix 0 refer to the bath temperature T_0. If $\rho S_0 \Delta T$ is denoted by Δp_{cor} the correction is found to be:

$$\frac{\Delta p - \Delta p_{\mathrm{cor}}}{\Delta p_{\mathrm{cor}}} = \tfrac{1}{2} \frac{C_0}{S_0} \frac{\Delta T}{T_0} + \ldots \quad (3)$$

where C_0 is the specific heat of the liquid at the working pressure. As the temperature difference required to create a fountain pressure of the order of 10 cm oil increases with decreasing bath temperature to about 100 millidegrees at a bath temperature of 1°K, and moreover as $C/S > 1$, the correction may be of the order of 10% at low temperatures.

3. *Measurements and results.* The fountain pressures were measured at bath temperatures between 1.17°K and the λ-temperature and at pressures up to about 25 atm. As the density of liquid helium as a function of temperature and pressure was known from the measurements of Keesom and Keesom [5]) the entropy per unit mass could be derived from our measurements. In a first approximation the entropy was determined by calculating the slopes of the curves Δp *versus* ΔT at $\Delta T = 0$. These entropy values were used in computing the corrections to Δp according to formula (3). From the graphs Δp_{cor} *versus* ΔT we derived the entropy in a second approximation, *etc.* At higher temperatures the correction was found with sufficient accuracy in one step, but at lower temperatures the process had to be repeated once more. A typical result is shown in fig. 2, where Δp_{cor} has been plotted *versus* ΔT for seven different external pressures at a bath temperature of 1.763°K. Within the experimental accuracy the points lie on straight lines and all lines meet at the origin. This is an indication that the experimental conditions for the measurements of Δp and ΔT were satisfied, especially, for instance, that the temperature gradients in the capillaries leading to the top of the cryostat were equal and that the superleak was of good quality. If the heat flow from the heater had caused a difference of the temperature gradient in these capillaries the lines would not have gone through the origin and if the heat leak through the superleak had been large, the curves Δp *versus* ΔT would have been bent over to the ΔT axis as has been shown in the early experiments of Mellink [7]). Such departures were indeed observed, the first when working without the spiral tube C and the second with an imperfect superleak.

Similar graphs as shown in fig. 2 were obtained for all temperatures except at the lowest temperature $T = 1.176$°K. Here the largest ΔT

amounts to about 80 millidegrees and hence the contribution of the third term on the right hand side of eq. (2) is no longer negligibly small; the correction due to this term being about 3%. In this case we therefore calculated the corrections in a modified way. The provisionally determined entropy at constant pressure was found to nearly satisfy the relation $S = AT^n$ over a not too large temperature range. From these analytic expressions for different pressures the coefficients of $(\Delta T)^2$ and $(\Delta T)^3$ were calculated and then plotted against pressure. The coefficients at the actual pressures could be determined from the graph obtained. This operation was

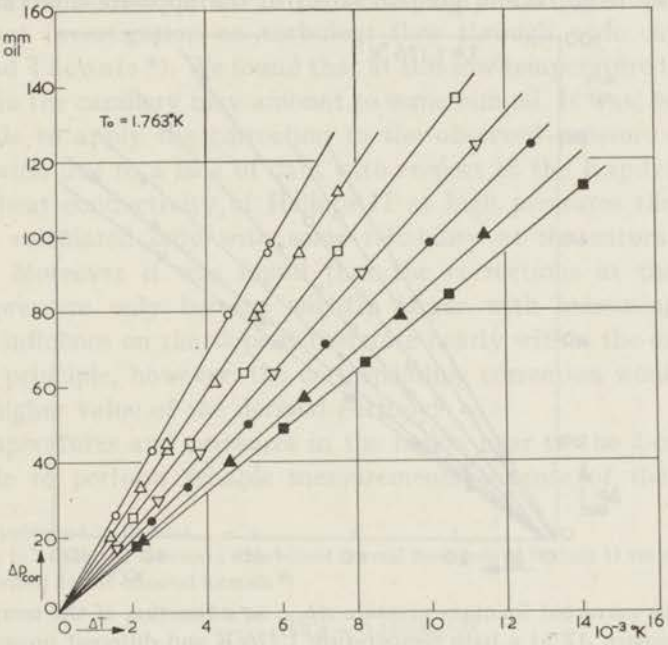

Fig. 2. The corrected fountain pressure Δp_{cor} as a function of the temperature difference ΔT at a bath temperature 1.763°K and different pressures
■: $P = 0.08$ atm ▽: $P = 12.17$ atm △: $P = 21.04$ atm
▲: $P = 3.85$ atm □: $P = 17.06$ atm ○: $P = 24.71$ atm
●: $P = 8.32$ atm

repeated a few times. The final results at 1.176°K are shown in fig. 3. In contrast to the graphs obtained at higher temperatures, this graph shows a remarkable deviation; the points nearly lie on straight lines but the lines do not meet at the origin, whereas the origin itself corresponds to the observed zero pressure difference at zero temperature difference. On extrapolating the lines the maximum deviation at the origin is found to be about 3 mm oil in the pressure difference corresponding to minus 2.5 millidegree in the temperature difference. Of course, these deviations cannot originate from the technique of calculation. At first sight one would be tempted to

conclude that the deviations are caused somewhere in the capillaries coming from the top of the cryostat where strong temperature gradients are present. However, the difference in weight of the helium columns corresponding to the deviation in Δp which must be explained, is equivalent to a column of about 1.5 cm liquid helium. This is a rather large difference which, moreover, should disappear at $\Delta T = 0$. The assumption that a difference in the heat leak from the top of the cryostat in the two capillaries would have caused this effect is, therefore, very unlikely. An influence of the heat flow from the heater on the temperature gradient in the capillary E, on the other hand, would give an effect in the opposite direction. For, in

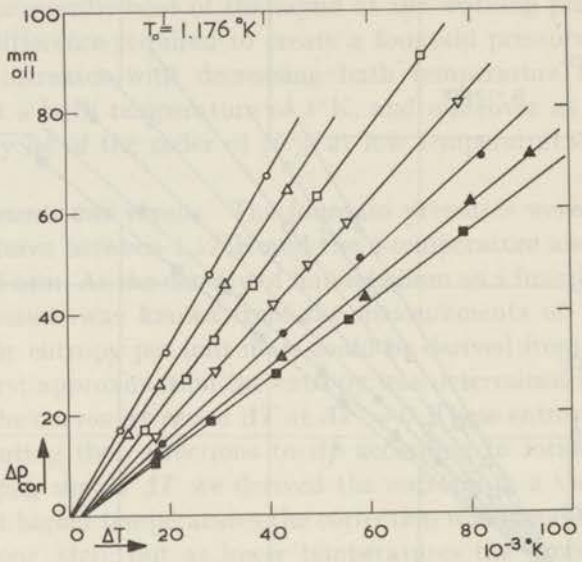

Fig. 3. The corrected fountain pressure Δp_{cor} as a function of the temperature difference ΔT at a bath temperature 1.176°K and different pressures
■: $P = 0.13$ atm ▽: $P = 12.08$ atm △: $P = 20.76$ atm
▲: $P = 2.48$ atm □: $P = 16.81$ atm ○: $P = 24.63$ atm
●: $P = 7.16$ atm

this case the mean density in the "higher" pressure capillary should be smaller than the mean density in the "lower" pressure capillary and such a difference gives rise to an increase in the pressure difference observed on the oil manometer. Furthermore, as a consequence of our method in determining ΔT, a deviation of T_1 from the bath temperature cannot enter into ΔT. Hence, a difference between the actual ΔT and the measured ΔT is possible only if a temperature gradient exists between the copper block B and the superleak (fig. 1). A temperature difference of 2.5 millidegree across a capillary of 2 cm length and 1 mm inside diameter implies a heat current of about 1.5 milliwatt, which is nearly half the maximum heat input at this temperature. This is almost impossible because the superleak then

would have to have had a hole of the order of $\frac{1}{2}$ mm diameter. Our conclusion is therefore that the deviation must be due to a fountain pressure originating from the heat flow in capillary C. The fountain pressure in the capillary would be opposite to the fountain pressure across the superleak and this would therefore result, indeed, in too small a pressure difference on the oil manometer. As was mentioned already in section 2, the fountain pressure arising from a laminar normal fluid flow in capillary C is an order of magnitude too small. The higher fountain pressure must arise, therefore, from a turbulent normal fluid flow. In order to lend weight to this argument we calculated the pressure gradient in the capillary starting from the results of a recent investigation on turbulent flow through wide capillaries by Staas and Taconis *). We found that at this low temperature the fountain pressure in the capillary may amount to some mm oil. It was, however, not worthwhile to apply the correction to the observed pressure differences, first, because due to a lack of data with respect to the Kapitza resistance and the heat conductivity of Helium II at high pressures the correction could be calculated only with some reliability at the saturated vapour pressure. Moreover it was found that the corrections at the saturated vapour pressure only become slightly larger with increasing ΔT. The resulting influence on the slope is therefore nearly within the experimental error. In principle, however, the corresponding correction would lead to a slightly higher value of the derived entropy.

At temperatures and pressures in the region near to the λ-curve it was impossible to perform reliable measurements because of the instability

*) To be published in Physica.

According to Staas and Taconis a turbulent normal fluid flow of Helium II through a capillary may be described by the classical formula [8])

$$\frac{16r^3\rho}{\eta_n^2}\,\mathrm{grad}\,p = 0.316(Re)^{1.75} \tag{4}$$

where r is the radius of the capillary, η_n the normal fluid viscosity, ρ the total density of the liquid and Re the Reynolds number. The Reynolds number $Re = 2r\rho v/\eta_n = 2r\varphi/\eta_n ST$ decreases over the tube length, because the heat flow density φ decreases. If the temperature difference between the helium inside and outside the tube at a distance x from the heater is ΔT and the boundary resistance including the resistance of the wall is R, the heat flow in the capillary may be determined from the equation:

$$\pi r^2 \frac{\mathrm{d}\varphi}{\mathrm{d}x} = -2\pi r \frac{\Delta T}{R}. \tag{5}$$

Moreover, as the heat conductivity of the liquid helium in the small range of the temperature variation ΔT approximately may be described with the equation:

$$\varphi = -A\left(\frac{\mathrm{d}T}{\mathrm{d}x}\right)^{\frac{1}{3}}. \tag{6}$$

with constant A, $\varphi(x)$ can be solved from eqs. (5) and (6). Substituting $\varphi(x)$ into eq. (4) and integrating over the tube length the fountain pressure is found, at least in a first approximation. Because Re decreases with increasing temperature and pressure, due to the increase of the entropy the correction is only of some importance at low temperatures and low pressures. This is also shown in fig. 3; the deviation disappears at high pressure.

of the pressure difference Δp. This instability originated for a deal from the insufficient control of the bath pressure. Moreover, oscillations of the oil levels due to vibration of the helium columns in the capillaries E, often appeared.

All our numerical data on pressure and entropy as obtained at different temperatures, together with the density values used are given in table I.

TABLE I

Experimental Values of the Entropy

P atm	ρ g/cm³	S J/g°K
$T = 1.176$ °K		
0.13	0.1447	0.0448
1.90	0.1476	0.0463
2.48	0.1484	0.0472
2.49	0.1484	0.0465
7.16	0.1550	0.0519
12.08	0.1606	0.0599
16.81	0.1653	0.0695
20.76	0.1687	0.0786
24.63	0.1718	0.0876
$T = 1.355$ °K		
0.28	0.1450	0.110
1.85	0.1476	0.111
4.54	0.1516	0.116
8.72	0.1570	0.126
12.63	0.1613	0.139
16.44	0.1650	0.153
20.53	0.1687	0.172
25.45	0.1728	0.200
$T = 1.501$ °K		
0.68[5]	0.1458	0.199
$T = 1.511$ °K		
0.43	0.1453	0.203
1.92	0.1478	0.207
4.52	0.1517	0.217
8.35	0.1567	0.233
12.14	0.1610	0.252
16.44	0.1653	0.282
20.45	0.1690	0.316
23.10	0.1713	0.342
25.79	0.1735	0.376
$T = 1.603$ °K		
0.66[5]	0.1458	0.285

P atm	ρ g/cm³	S J/g°K
$T = 1.608$ °K		
0.05	0.1448	0.293
0.67	0.1458	0.294
1.88	0.1478	0.299
4.56	0.1518	0.312
8.35	0.1568	0.334
12.40	0.1614	0.361
17.65	0.1667	0.415
22.25	0.1709	0.473
26.30	0.1743	0.538
$T = 1.702$ °K		
0.50	0.1455	0.398
$T = 1.703$ °K		
0.53	0.1456	0.405
1.99	0.1481	0.410
4.52	0.1519	0.425
8.53	0.1572	0.453
12.48	0.1618	0.497
17.62	0.1671	0.565
21.50	0.1707	0.638
25.50	0.1743	0.729
$T = 1.763$ °K		
0.08	0.1448	0.484
1.03	0.1465	0.489
3.85	0.1510	0.508
8.32	0.1571	0.549
12.17	0.1616	0.599
17.06	0.1668	0.677
21.04	0.1707	0.764
24.71	0.1742	0.864
$T = 1.806$ °K		
0.85	0.1462	0.553
$T = 1.808$ °K		
0.90	0.1463	0.561
2.39	0.1488	0.571
4.55	0.1521	0.590
8.36	0.1572	0.631
12.50	0.1621	0.693
16.67	0.1666	0.775

P atm	ρ g/cm³	S J/g°K
$T = 1.855$ °K		
0.16	0.1450	0.645
1.46	0.1474	0.658
3.93	0.1513	0.678
7.58	0.1564	0.720
11.65	0.1614	0.786
15.60	0.1658	0.875
17.33	0.1676	0.920
$T = 1.904$ °K		
0.30	0.1454	0.743
1.92	0.1482	0.755
4.50	0.1523	0.784
8.08	0.1572	0.838
14.75	0.1652	0.985
$T = 1.947$ °K		
0.07	0.1450	0.832
1.43	0.1475	0.847
3.89	0.1515	0.874
6.98	0.1560	0.923
10.75	0.1609	1.011
$T = 2.001$ °K		
0.04	0.1450	0.968
1.50	0.1477	0.985
4.36	0.1524	1.028
8.07	0.1578	1.110
$T = 2.044$ °K		
0.05	0.1451	1.083
1.43	0.1477	1.101
$T = 2.054$ °K		
0.05	0.1452	1.122
2.52	0.1496	1.168
3.25	0.1509	1.182

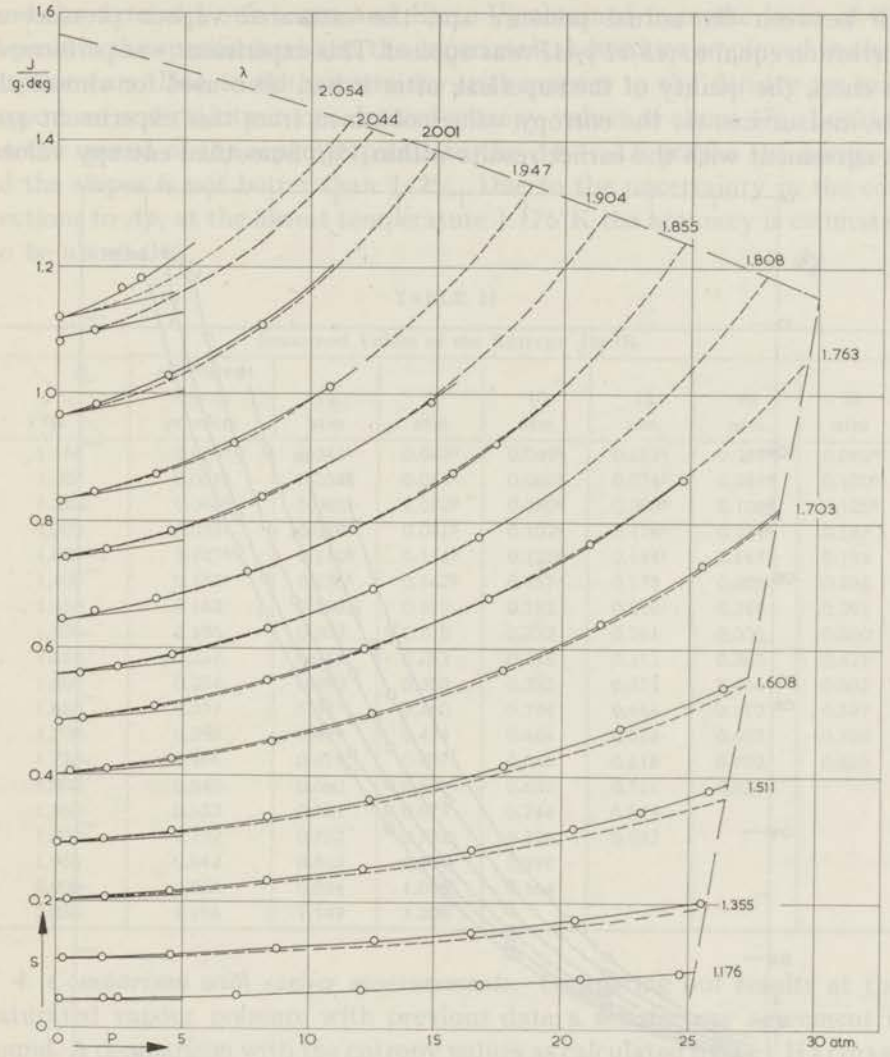

Fig. 4. The entropy S as a function of the pressure P at different temperatures
Points and solid curves: present results
Dotted curves: calculated from the data of Keesom and Keesom and fitted at $P = 0$.
The slopes drawn at $P = 0$ correspond to the coefficients of expansion according to Atkins and Edwards.

Fig. 4 shows the entropy *versus* the pressure. The solid lines are smoothed curves corresponding to the different temperatures which are indicated in the graph. The entropy as a function of temperature at different pressures as derived from fig. 4, is presented in fig. 5. The extra points in fig. 5 on the curve corresponding to the saturated vapour pressure were obtained from a special experiment at low pressures only. For the difference

ΔP between the actual pressure and the saturated vapour pressure a correction equal to $(\partial S/\partial P)_T \Delta P$ was applied. This experiment was performed to check the quality of the superleak after it had been used for almost all the measurements; the entropy values obtained from this experiment are in agreement with the earlier results within 1%. Smoothed entropy values

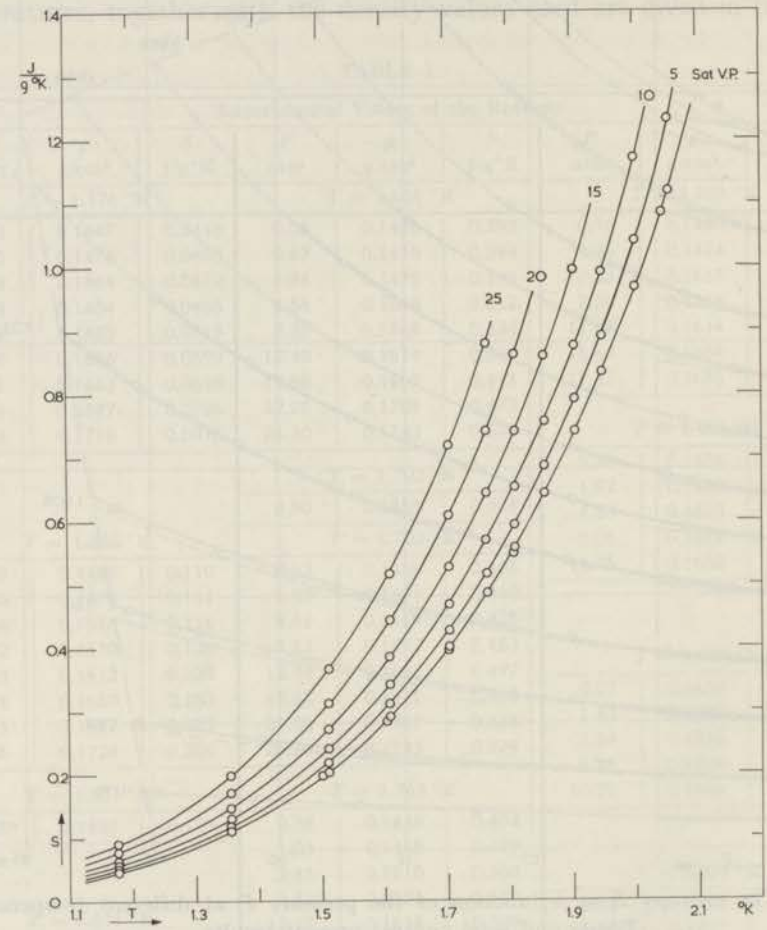

Fig. 5. The entropy S as a function of the temperature T at different pressures. The numbers attached to the curves indicate the pressure P in atm.

derived from our results are given in table II. The temperature values in the tables are based on the 1958 temperature scale. We already mentioned that we consistently used the density data of Keesom and Keesom. There is, however, a discrepancy of about 0.6% between the Keesom and Keesom density values obtained by extrapolation to the saturated vapour pressure and the more recent data on the liquid density at the saturated vapour pressure of Kerr [9]). Furthermore, at the λ-curve there is a discrepancy varying up to about 1.5% between the data of Keesom and Keesom [10])

and the data of Lounasma and Kojo [11]) obtained from the locus of the λ-peak in the specific heat and the experimental densities employed in their experiments. Due to the uncertainty with respect to the density we may expect an uncertainty in our derived entropy values of about 1%. Looking at the spread of the separate points in the $\Delta p - \Delta T$ graphs the accuracy of the slopes is not better than 1–2%. Due to the uncertainty in the corrections to Δp, at the lowest temperature 1.176°K the accuracy is estimated to be about 3%.

TABLE II

Smoothed Values of the Entropy J/g °K							
P / T°K	saturated vapour pressure	2½ atm	5 atm	10 atm	15 atm	20 atm	25 atm
1.150	0.039⁵	0.041⁰	0.043⁰	0.049⁰	0.057⁵	0.068⁰	0.080⁰
1.200	0.051⁵	0.053⁵	0.056⁰	0.063⁵	0.074⁰	0.086⁰	0.100⁰
1.250	0.066⁵	0.068⁵	0.072⁰	0.080⁵	0.093⁰	0.108⁰	0.125⁵
1.300	0.085⁵	0.088⁰	0.091⁵	0.102⁰	0.116⁰	0.134⁵	0.157
1.350	0.107⁵	0.110⁵	0.114⁵	0.127⁰	0.144⁰	0.167	0.194
1.400	0.132⁵	0.136⁵	0.142⁰	0.157	0.178	0.205	0.238
1.450	0.162	0.166	0.173	0.192	0.216	0.248	0.291
1.500	0.196	0.202	0.210	0.232	0.261	0.300	0.350
1.550	0.237	0.244	0.253	0.278	0.313	0.360	0.421
1.600	0.284	0.292	0.303	0.332	0.374	0.430	0.502
1.650	0.337	0.347	0.360	0.394	0.444	0.510	0.597
1.700	0.398	0.409	0.424	0.464	0.524	0.602	0.709
1.750	0.466	0.479	0.497	0.545	0.615	0.709	0.838
1.800	0.545	0.560	0.581	0.637	0.721	0.836	
1.850	0.633	0.651	0.677	0.744	0.844		
1.900	0.732	0.752	0.782	0.863	0.982		
1.950	0.842	0.865	0.900	0.998			
2.000	0.963	0.994	1.035	1.164			
2.050	1.105	1.149	1.209				

4. *Comparison with earlier measurements.* Comparing our results at the saturated vapour pressure with previous data a satisfactory agreement is found. A comparison with the entropy values as calculated by Ter Harmsel and Van Dijk *) from the specific heat data of Kramers, Wasscher and Gorter [12]), and Keesom and Keesom [13]), based on the 1958 temperature scale, is shown in fig. 6. The deviations are within experimental accuracy. We note again that the curve shifts upwards over about 0.6% when the density values of Kerr [9]) are used in the calculation of the entropy which, however, would give poorer agreement.

From the specific heat measurements at the saturated vapour pressure of Lounasma and Kojo [11]) above 1.45°K, entropy differences can be derived. A comparison has been made by fitting the data of Lounasma and Kojo to our entropy value at 1.6°K. The remaining relative deviations

*) To be published in Physica.

from our smoothed values are also shown in fig. 6. The agreement is good.

From the data on the coefficient of thermal expansion of the liquid at the saturated vapour pressure of Atkins and Edwards [14]) one can calculate $(\partial S/\partial P)_T = -(\partial V/\partial T)_P$ *i.e.* the slope of the curves $S(P)$ at constant temperature at $P = 0$. The calculated slopes are drawn in fig. 4. Although this comparison is not very sensitive, one may see that the slopes are compatible with our results.

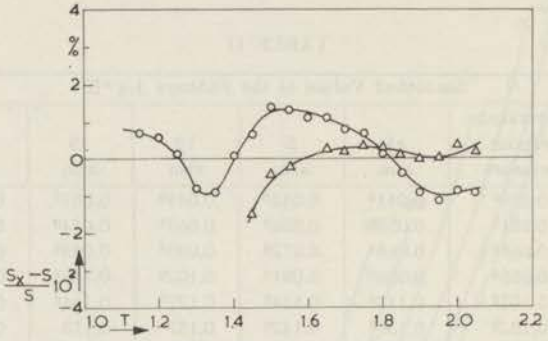

Fig. 6. The relative difference between the present entropy values (S) and the entropy values derived from the specific heat (S_x) at saturated vapour pressure, plotted against the temperature T.
○: S_x calculated by Ter Harmsel and Van Dijk.
△: S_x Lounasma and Kojo, fitted at 1.6°K.

To study the dependence of the entropy upon the pressure we calculated from the data of Keesom and Keesom [15]) the entropy increase as a function of pressure:

$$S(P) - S(0) = \int_0^P \frac{1}{\rho^2}\left(\frac{\partial \rho}{\partial T}\right)_P \mathrm{d}P$$

and the entropy increase as a function of density:

$$S(\rho) - S(\rho_0) = \int_{\rho_0}^{\rho} \frac{1}{\rho^2}\left(\frac{\partial P}{\partial T}\right)_\rho \mathrm{d}\rho.$$

In this calculation we also included the data of Atkins and Edwards on the coefficients of expansion at the saturated vapour pressure. The dotted curves in fig. 4 represent the averaged value of $S(P)$ resulting from these calculations, substituting for $S(0)$ our smoothed entropy values at the saturated vapour pressure. Taking into account the accuracy of these calculations the agreement within 5% of the entropy increase as found between 1.7 and 2.0°K is very satisfactory. At lower temperatures the deviations increase up to about 20% of the entropy increase. It seems to us that these deviations are larger than we should expect with respect to the

accuracy of the calculations. The discrepancy disappears, however, if relatively small corrections in the density are applied.

After we finished these calculations data on the specific heat of liquid helium under pressure were published by Lounasma and Kojo [11]). The specific heat was measured from about 1.5°K up to above the λ-curve at seven different densities. Apart from a constant, the entropy as a function of temperature at constant density can be calculated from these data. For lack of entropy data below the λ-curve Lounasma and Kojo fitted the

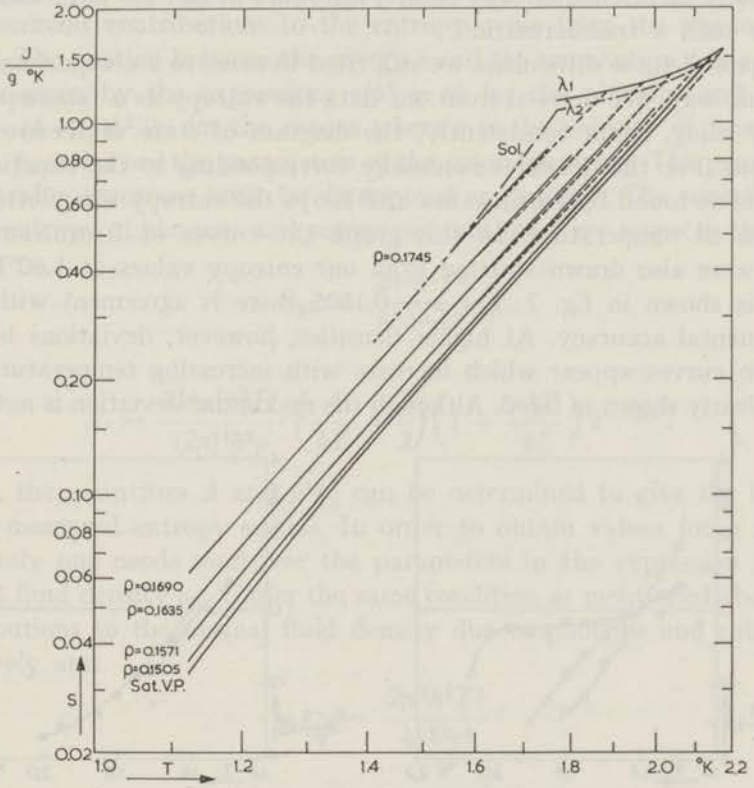

Fig. 7. The entropy S as a function of the temperature T at different densities.
Solid curves: present results.
Dotted curves: Lounasma and Kojo, fitted at 1.6°K.
λ_1: λ-curve according to Lounasma and Kojo.
λ_2: λ-curve according to Keesom and Keesom

entropy to the values at 2.5°K of Hill and Lounasma [16]). But due to the λ-peak in the specific heat and the corresponding strong decrease of the entropy with decreasing temperature below the λ-curve the accuracy of the absolute values becomes gradually poorer at low temperatures. It is therefore preferable to start from absolute entropy values at a temperature as far as possible below the λ-curve. Hence, by combining our results with the

results of Lounasma and Kojo it should be possible to construct the entropy diagram more precisely in the entire He II region above 1.2°K. Unfortunately, however, in the experiment of Lounasma and Kojo only the experimental densities were determined and the pressure was not measured. Because the density is, relatively, an insensitive quantity with respect to its dependence on temperature and pressure, the diagram of state must be known with great precision when a transformation is made from density to pressure. The relatively small discrepancies in the density data, which were mentioned already before, introduce in fact too large uncertainties for such a transformation.

In spite of these difficulties we still tried to come to a comparison in the following way. We derived from our data the entropy as a function of the density using, again consistently, the diagram of state of Keesom and Keesom. For the densities nominally corresponding to the experimental densities as found by Lounasma and Kojo the entropy was plotted as a function of temperature. In this graph the curves of Lounasma and Kojo were also drawn starting from our entropy values at 1.60°K. The result is shown in fig. 7. For $\rho = 0.1505$ there is agreement within the experimental accuracy. At higher densities, however, deviations between the two curves appear which increase with increasing temperature as is more clearly shown in fig. 8. Although the maximum deviation is not larger

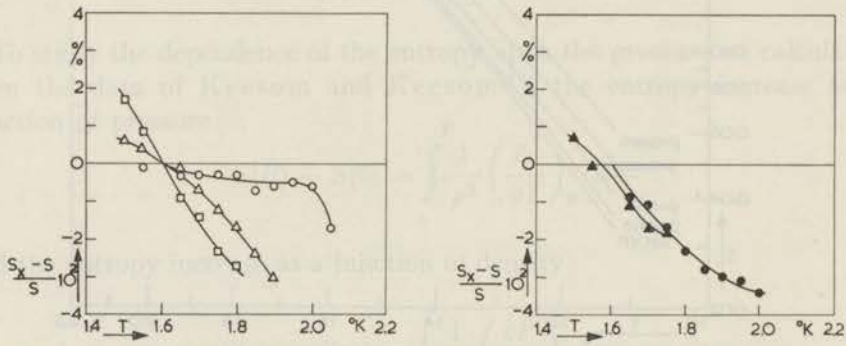

Fig. 8. The relative difference between the present entropy values (S) and the entropy values derived from the specific heat data of Lounasma and Kojo fitted at 1.6°K (S_x) plotted against the temperature T for different densities.

○: $\rho = 0.1505$ g/cm³ □: $\rho = 0.1690$ g/cm³
●: $\rho = 0.1571$ g/cm³ ▲: $\rho = 0.1745$ g/cm³
△: $\rho = 0.1635$ g/cm³

than 4% it is plausible that systematic deviations are involved originating from a small systematic error in the fit by means of the density. The uncertainty in the λ-curve due to the discrepancy in the density data is for illustration also shown in fig. 7; λ_1 is the λ-curve according to Lounasma and Kojo; λ_2 is the λ-curve derived from the density data of Keesom and

Keesom. We still note that the entropy curve of Lounasma and Kojo corresponding to $\rho = 0.1778$ has been omitted here because a too small part of it lies in the Helium II region to make a reliable fit to our entropy values.

5. *The parameters of the energy momentum spectrum.* We may compare our results with the expressions for the entropy derived on the basis of the energy momentum spectrum of the elementary excitations in Helium II as proposed by Landau. At temperatures not too near the λ-temperature the dominant contributions to the entropy come from the phonons and rotons. The relation between the energy ε and the momentum p is approximately given by the expressions $\varepsilon(p) = cp$ for the phonons and $\varepsilon(p) = \Delta + (p - p_0)^2/2\mu$ for the rotons where c is the velocity of first sound and Δ, p_0 and μ are the parameters of the roton spectrum. The parameters of the roton spectrum must be determined empirically. The contributions to the entropy of phonons and rotons per unit mass are respectively:

$$S_{ph} = \frac{2\pi^2 k^4 T^3}{45\hbar^3 \rho c^2} \tag{7}$$

and

$$S_r = \frac{2k^{\frac{1}{2}}\mu^{\frac{1}{2}}p_0^2 T^{\frac{1}{2}}}{(2\pi)^{\frac{1}{2}}\hbar^3 \rho}\left(\frac{\Delta}{kT} + \frac{3}{2}\right)\left(1 + \frac{\mu kT}{p_0^2}\right) e^{-\Delta/kT}. \tag{8}$$

Hence, the quantities Δ and $\mu^{\frac{1}{2}}p_0^2$ can be determined to give the best fit to the measured entropy values. In order to obtain values for μ and p_0 separately one needs moreover the parameters in the expression for the normal fluid density ρ_n. Under the same condition as mentioned above the contributions to the normal fluid density due to phonons and rotons respectively are:

$$\rho_{n,ph} = \frac{2\pi^2 k^4 T^4}{45\hbar^3 c^5} \tag{9}$$

and

$$\rho_{n,r} = \frac{2\mu^{\frac{1}{2}}p_0^4}{3(2\pi)^{\frac{1}{2}}k^{\frac{1}{2}}\hbar^3 T^{\frac{1}{2}}}\left(1 + 6\,\frac{\mu kT}{p_0^2}\right) e^{-\Delta/kT}. \tag{10}$$

From a fit of the parameters in eq. (10) to the measured ρ_n values the quantities Δ and $\mu^{\frac{1}{2}}p_0^4$ can be determined. If the values of Δ, "independently" derived from the data on S and ρ_n respectively, be in agreement, the parameters p_0 and μ may be derived from the quantities $\mu^{\frac{1}{2}}p_0^2$ and $\mu^{\frac{1}{2}}p_0^4$. We now have data available to perform these calculations for various pressures up to 25 atm.

S_{ph} was calculated using the data on the velocity of first sound of Atkins and Stasior [17]) and the data on the density of Keesom and Keesom [5]).

We note that at constant temperature S_{ph} decreases with increasing pressure similar to the entropy of an ordinary liquid, whereas S_r increases with increasing pressure due to the shift of the λ-point to lower temperatures. The quantities Δ and $\mu^3 p_0^2$ were determined by inserting $S_r = S - S_{ph}$ into eq. (8), using our present data on entropy and, for a comparison, also the entropy data as calculated by Ter Harmsel and Van Dijk for the saturated vapour pressure. The values of Δ obtained from eq. (8) are tabulated in table III. We note that only data at temperatures below 1.3°K

TABLE III

The energy gap Δ at different pressures

P atm	0	$2\frac{1}{2}$	5	10	15	20	25
Δ/k °K	8.9^0	8.6^5	8.4^5	8.0^0	7.6^0	7.2^5	6.9^5

were used in the calculation; firstly, because the temperature at which deviations from eqs. (7)–(10) occur decreases with increasing pressure due to the decrease of the λ-temperature and moreover because., in fact, Δ also depends on temperature as has been shown in the direct measurements of the energy momentum spectrum by means of inelastic scattering of neutrons. The values of Δ are shown plotted in fig. 9 together with the values obtained

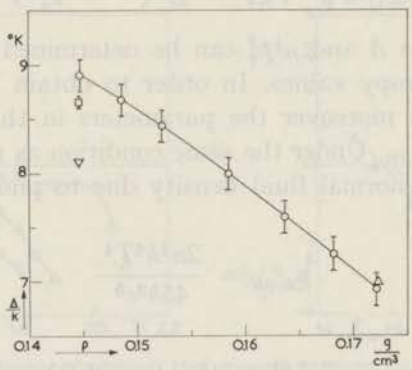

Fig. 9. The dependence of the energy gap Δ on the density ρ.
○ : derived from entropy
▽ : Palevsky *e.a.* at 1.4°K
□ : Yarnell *e.a.* at 1.1°K
△ : Henshaw and Woods at 1.1°K

from the neutron experiments of Palevsky, Otnes, Larsen, Pauli and Stedman [18] ($\Delta = 8.1$°K at 1.4°K and S.V.P.), Yarnell, Arnold, Bendt and Kerr [19] ($\Delta = 8.65 \pm 0.04$°K at 1.1°K and S.V.P.) and Henshaw and Woods [20] ($\Delta = 8.65$°K at 1.1°K and S.V.P.; $\Delta = 7.00$°K at 1.1°K and 25.3 atm.). At the saturated vapour pressure the value of Δ obtained from

the entropy data is higher than the direct measured values. However, in our calculation only the contributions to the entropy due to the phonons and rotons have been taken into account. Calculations by Bendt, Cowan and Yarnell [21]), based on the energy momentum spectrum at the saturated vapour pressure, show that the contribution due to the remaining regions of the spectrum cannot be neglected at temperatures above 0.8°K. With the division in momentum intervals as made by Bendt *e.a.* the relative contributions of the intervals in question were found to vary nearly linearly from 0% at about 0.8°K up to 19% of the total entropy at 1.8°K. Such a correction applied to S_r in our calculation gives rise to a correction of minus 0.3°K in Δ. Hence, the discrepancy between the value of Δ derived from entropy and the value of Δ as measured by Yarnell *e.a.* and Henshaw *e.a.* at the saturated vapour pressure may be explained in this way. The value of Δ as found by Palevsky *e.a.*, however, is beyond this correction. In view of the abovementioned considerations the agreement of the values for Δ at 25 atm seems surprisingly good. It is possible that at high pressures the correction in S_r varies less strongly with temperature in the small temperature range involved in our calculation.

Atkins and Edwards [14]) found $(\rho/\Delta)(\partial\Delta/\partial\rho) = -0.57$ from the data on the coefficient of expansion at the saturated vapour pressure, using the entropy data of Hercus and Wilks [22]). When this calculation is performed using the Leiden entropy data $(\rho/\Delta)(\partial\Delta/\partial\rho) = -0.75$ is found. Taking into account that the pressure dependence of the velocity of first sound has been neglected in this calculation, which gives rise to a correction of the order of 10%, the result appears to be roughly in agreement with our data, from which we derive $(\rho/\Delta)(\partial\Delta/\partial\rho) \approx -0.9$. It is clear that entropy data down to lower temperatures are required to obtain accurate values of Δ. The accuracy of $\pm$ 0.15°K indicated in fig. 9, is the estimated accuracy of the calculation apart from systematic errors.

The normal fluid density was calculated using the formula:

$$\rho_n = \frac{\rho}{1 + \frac{u_2^2 \left(\frac{\partial S}{\partial T}\right)_V}{S^2}}$$

and the data on the velocity of second sound (u_2) of Maurer and Herlin [23]) and of Elliot and Fairbank *) the data on ρ of Keesom and Keesom [5]) and the present entropy data. After inserting $\rho_{n,r} = \rho_n - \rho_{n,ph}$ into eq. (10) it was found that the values of Δ obtained from eq. (8) indeed were compatible with these data on $\rho_{n,r}$ at all pressures in the considered temperature range. It appeared, however, that Δ could be determined more accurately

*) We thank Dr. S. D. Elliott and Dr. H. E. Fairbank for giving us their data.

from the data on S than from the data on ρ_n.*) Therefore the quantity $\mu^{\frac{1}{2}}p_0^4$ was determined from eq. (10) by starting with the values for Δ as obtained from eq. (8).

As Δ does not enter in the expression for p_0 exponentially and moreover as the errors in S_r and $\rho_{n,r}$ due to the contributions of the excitations which have been neglected partly cancel, p_0 is presumably determined within a few percent in this way. In fig. 10 $p_0/\hbar$ is shown plotted *versus* density. At

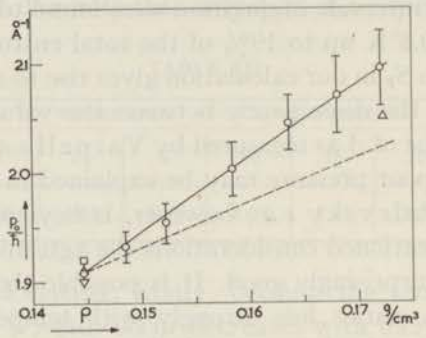

Fig. 10. The dependence of the parameter p_0 on the density ρ.
○ : derived from entropy and velocity of second sound.
▽ : Palevsky *e.a.*
□ : Yarnell *e.a.*
△ : Henshaw and Woods

The dotted curve corresponds to $\frac{\rho}{p_0}\frac{dp_0}{d\rho} = 1/3$.

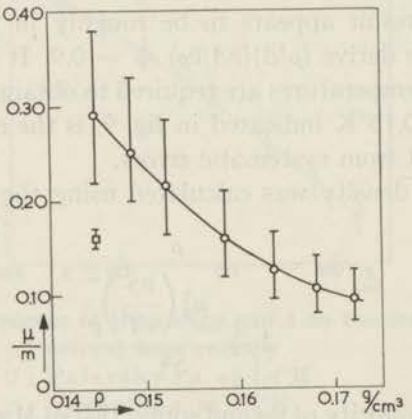

Fig. 11. The dependence of the parameter μ on the density ρ.
○ : derived from entropy and velocity of second sound
□ : { Palevsky *e.a.*
Yarnell *e.a.*

*) The situation is different for the saturated vapour pressure, because more data down to lower temperatures are here available. By using the recent data on the velocity of second sound of Peshkov [24]) combined with the Leiden entropy data down to 1°K a more accurate value for Δ/k can be derived. It is surprising that this calculation, without any correction, gives $\Delta/k = 8.65$°K.

the saturated vapour pressure there is agreement with the directly measured value within the experimental error. At high pressures, however, the discrepancy is slightly beyond this range.

The accuracy of the μ-values obtained from the data on S and ρ_n is very poor as may be seen in fig. 11, where μ/m is shown plotted against density; m is the mass of the helium atom; $m = 6.65 \times 10^{-24}$ g. The errors indicated in the figure are mainly due to the estimated error of $\pm$ 0.15°K in Δ. If to the value of Δ at saturated vapour pressure a correction of -0.3°K is applied, as has already been suggested the corresponding value of μ/m decreases to 0.17 and then agreement is obtained with the directly measured value: $\mu/m = 0.16 \pm 0.01$.

Although the numerical data derived for Δ, p_0 and μ are not very accurate the dependence on density as shown in figs. 9–11 is at least qualitatively in agreement with the expectations on the basis of Feynman's theory [25]). According to this theory the relation between energy and momentum may be written:

$$\varepsilon(p) = \frac{p^2}{2mS(k)}$$

where $S(k)$, the liquid structure factor, is the Fourier transform of the radial distribution function, which gives the probability that an atom will be found at a fixed distance from another atom, as a function of that distance. The maximum in $S(k)$, which nearly corresponds to the minimum in $\varepsilon(p)$, will therefore be found at a wave number $p/\hbar$, corresponding to the inverse of the atomic distance in the liquid. One should therefore expect p_0 to be proportional in a first approximation to $\rho^{\frac{1}{3}}$. The dotted curve in fig. 10 represents this relation starting from $p_0/\hbar = 1.91$ Å^{-1} at S.V.P. The maximum deviation from this curve is 4%. Further, one should expect that the first maximum of the radial distribution function would be sharper and higher if the local order in the liquid increases. This gives rise to a decrease of Δ and μ as was indeed found.

REFERENCES

1) *e.g.*: Kapitza, P. L., J. Phys. U.S.S.R. **5** (1942) 59.
Meyer, L. and Mellink, J. H., Commun. Kamerlingh Onnes Lab., Leiden No. 272*b*; Physica **13** (1947) 197.
Van den Meijdenberg, C. J. N., Taconis, K. W., Beenakker, J. J. M. and Wansink, D. H. N., Commun. No. 295*c*; Physica **20** (1954) 157.; Introduction.
Bots, G. J. C. and Gorter, C. J., Commun. No. 304*b*; Physica **22** (1956) 503.
Bots, G. J. C. and Gorter, C. J., Commun. No. 320*a*; Physica **26** (1960) 337.
2) London, F., J. Phys. Chem. **43** (1939) 49; Landau, L. D., J. Phys. U.S.S.R. **5** (1941) 71.
3) *e.g.* Kapitza, P. L., J. Phys. U.S.S.R. **4** (1941) 181.
Beenakker, J. J. M., Taconis, K. W., Lynton, E. A., Dokoupil, Z. and Van Soest, G., Commun. No. 289*a*; Physica **18** (1952) 433.
4) Keesom, W. H., Saris, B. F. and Meyer, L., Commun. No. 260*a*; Physica **7** (1940) 817.
Keesom, W. H., Helium. Elsevier, Amsterdam 1942, p. 286.

5) Keesom, W. H. and Keesom, A. P., Commun. Suppl. No. 76*b*; Physica **1** (1933) 128.
Keesom, W. H., Helium. Elsevier, Amsterdam 1942, p. 245.
6) Brewer, D. F. and Edwards, D. O., Proc. roy. Soc. **A 251** (1959) 247.
7) Mellink, J. H., Commun. No. 272*a*; Physica **13** (1947) 180.
8) Schlichting, H., Boundary Layer Theory, Pergamon Press, London, 1955, p. 401.
9) Kerr, E. C., J. Chem. Phys. **26** (1957) 511.
10) Keesom, W. H., Helium. Elsevier, Amsterdam 1942, p. 226.
11) Lounasma, O. V. and Kojo, E., Ann. Acad. Scient. Fennicae **A** VI **36** (1959).
12) Kramers, H. C., Wasscher, J. D. and Gorter, C. J., Commun. No. 288*c*; Physica **18** (1952) 329.
13) Keesom, W. H. and Keesom, A. P., Commun. No. 221*d*; Proc. roy. Acad. Amsterdam **35** (1932) 736.
14) Atkins, K. R. and Edwards, M. H., Phys. Rev. **97** (1955) 1429.
15) Keesom, W. H. and Keesom, A. P., Commun. No. 224*d*, *e*; Proc. roy. Acad. Amsterdam **36** (1933) 482, 612.
16) Hill, R. W. and Lounasma, O. V., Proc. Vth Int. Conf. on Low Temp. Phys., Madison 1957, p. 48; Lounasma, O. V., Thesis Oxford, 1958.
17) Atkins, K. R. and Stasior, R. A., Canad. J. Phys. **31** (1953) 1156.
18) Palevsky, H., Otnes, K., Larsson, K. E., Pauli, R. and Stedman, R., Phys. Rev. **108** (1957) 1346; Palevsky, H., Otnes, K. and Larsson, K. E., Phys. Rev. **112** (1958) 11.
19) Yarnell, J. L., Arnold, G. P., Bendt, P. J. and Kerr, E. C., Phys. Rev. **113** (1959) 1379.
20) Henshaw, D. G. and Woods, A. D. B., Programme VIIth Int. Conf. on Low Temp. Phys. Toronto 1960, p. 64.
Henshaw, D. G., Phys. Rev. Letters **1** (1959) 127.
21) Bendt, P. J., Cowan, R. D. andYarnell, J. L., Phys. Rev. **113** (1959) 1386.
22) Hercus, G. R. and Wilks, J., Phil. Mag. **45** (1954) 1163.
23) Maurer, R. D. andHerlin, M. A., Phys. Rev. **82** (1951) 329.
24) Peshkov, V. P., J. eksp. teor. Fiz. U.S.S.R. **38** (1960) 799; Soviet Phys. JETP. **11** (1960) 580.
25) See *e.g.* Feynman, R. P., Progress in Low Temp. Phys. (Edited by C. J. Gorter) Vol *I*, Chapter *II*. North Holland Publishing Co., Amsterdam, 1955.

CHAPTER II

THE INFLUENCE OF ^{3}He ON FILM FLOW

Synopsis

The isothermal flow of the film in equilibrium with liquid mixtures of ^{3}He and ^{4}He was investigated in the temperature range between 1.3°K and the λ-temperature. The flow rate was found to be dependent on the temperature, the concentration and the height of the film above the liquid level, but independent of the pressure head. The results can not be described with the simple formula, suggested by Esel'son *e.a.*: $\sigma = A\rho_s/\rho$, where A is a constant. The variation of the flow rate with the height of the film appears to depend on both temperature and concentration.

Various flow measurements, including the present one, are considered in some detail in terms of the two fluid model.

1. *Introduction.* Many experiments have been done to study the flow properties of the film of pure ^{4}He and several authors have summarized and discussed the various results of these experiments. We refer to the most recent review articles for a detailed discussion of the experimental and theoretical features of the pure ^{4}He film [1]).

Our investigation deals with the influence of ^{3}He on the film behaviour. Not so very much was known on this subject when we started our experiment. Inghram, Long and Meyer (1955)[2]) investigated the distribution coefficient between film and unsaturated vapour. They found the distribution coefficient equal to the distribution coefficient between bulk liquid and saturated vapour. This result leads to the conclusion that, thermodynamically, there is no appreciable difference between film liquid and bulk liquid. Therefore it seems also reasonable to assume that the composition of the saturated film is equal to the composition of the bulk liquid when the vapour which is in equilibrium with the bulk liquid and the film, is homogeneous.

A few measurements on film flow have been made by Esel'son, Lazarew and Lifshitz (1950)[3]) and they report some data obtained with mixtures of 0.03% and 1,5% ^{3}He *). Their apparatus consists of two capillaries of different length, connected at the upper end. When the two capillaries contain an equal quantity of liquid (initial state), there is a difference in

*) We became aware of the experimental results of Esel'son *e.a.* after we started our experiment.

height of the liquid levels which gives rise to a film flow along the inside walls, from the capillary with the highest liquid level to the other one. The transfer of ^{4}He by the film, however, produces a concentration difference and hence a vapour pressure difference. The superfluid flow through the film will therefore be accompanied by a flow of ^{3}He through the vapour. At a fixed temperature and for small concentration differences the flow rate through the vapour is proportional to the pressure difference and in consequence to the concentration difference, the constant of proportionality being some measure of the flow resistance. Film flow, however, only occurs when the osmotic pressure difference due to the concentration difference is smaller than the hydrostatic pressure head. Owing to this condition a minimum value for the ratio of gas transfer and film transfer is required in order to maintain the film transfer. If the transfer rate of the film is large, the transfer rate of ^{3}He must be correspondingly large. The gas flow is limited, however, because the flow resistance is different from zero. Therefore, the film transfer rate can be measured in this way only if it is below a certain critical value, determined by the dimensions of the apparatus. Because of this restriction, with their apparatus Esel'son *e.a.* could only measure the film transfer rate in the direct vicinity of the lambda temperature, where the transfer rate of the film is very small. The transfer rate with the mixture of 1,5% ^{3}He was found to be slightly lower than that of the mixture of 0.03% ^{3}He, "in qualitative agreement with the increase of ρ_n/ρ by the presence of ^{3}He". Esel'son, Shvets and Bablidze [4]) extended these measurements in 1958 to mixtures up to 10% ^{3}He in the temperature range $T_\lambda - 0.04°\mathrm{K} < T < T_\lambda$. They state that the transfer rate of the film is proportional to the superfluid fraction ρ_s/ρ, the constant of proportionality being 3.2×10^{-5} cm^2/s; but in our opinion this relation does not describe their results adequately, as will be shown in section 4.

Some other experiments have been performed which deal with the flow of the film in equilibrium with a liquid mixture. We may mention the experiments of Daunt, Probst, Johnston, Aldrich and Nier (1947) [5]), Hammel and Schuch (1952) [6]) and Wansink and Taconis (1957) [7]). In these experiments a superleak has been placed above the surface of the liquid mixture and the film flows from the liquid to the superleak. In any of these cases the film takes part in the transfer as the film path is part of the total path of the flow. But the conditions in and near the superleak must be considered in detail in order to conclude whether the transfer rate is determined by the film or by the superleak. Daunt *e.a.* did not intend to investigate the influence of ^{3}He on the flow rate of the film in the experiment mentioned above. As they used mixtures of very low concentrations the influence of the ^{3}He on the transfer rate would not have been observable in this case. Closer investigation of the conditions in the experiments of Hammel and Schuch and of Wansink and Taconis revealed that not

the film, but the phenomena in the superleak dominated in determining the flow rate. This will be discussed in more detail in section 6.

We may still remark however, that the superfluid part of a mixture comprises ^{4}He atoms only. Superfluidity of ^{3}He has never been observed and, as will also be shown in section 6, the experiments dealing with bulk liquid flow of mixtures give no indication that ^{3}He participates in superfluid flow. When considering the flow of the saturated film in equilibrium with a mixture, we may consequently assume that the flow deals with moving ^{4}He only. Hence, the transfer rate σ will be governed by the superfluid fraction ρ_s/ρ, the velocity of the superfluid v_c and the thickness of the film d. Just as for the flow of a film of pure ^{4}He, we may write

$$\sigma = \frac{\rho_s}{\rho} v_c d. \tag{1}$$

In section 2 we will describe our method for measuring the film flow in equilibrium with mixtures. In sections 3 and 4 we discuss our measurements and results. The flow phenomena occurring in our measurements are discussed in more detail in section 5; and the results of the flow measurements, mentioned before, are considered more accurately in section 6.

2. *Apparatus and method.* A schematic diagram of the apparatus is shown in fig. 1. The lower vessel A is a glass capillary of accurately known

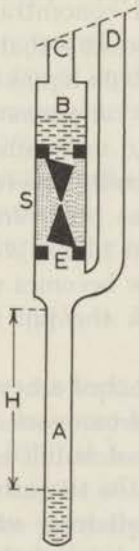

Fig. 1. Apparatus.

length and inside diameter. The upper vessel B is connected to A by a superleak S. The superleak consists of jewellers rouge powder compressed into a stainless steel capillary. The powder is kept together between needles,

which have been pushed in it and are fixed by small brass caps soldered to the ends of the capillary.

The caps have a bore with an inside diameter of about 1.2 mm. (see E in fig. 1). The glass capillary is connected to the superleak by means of a platinum-glass seal. The stainless steel capillaries C and D, with an inside diameter of 0.85 and 1.05 mm respectively lead to the top of the cryostat, where both are connected to a differential oil manometer and to a Toepler system.

Initially a ^{3}He–^{4}He mixture is condensed in A. When a mixture of higher concentration is condensed in B an osmotic pressure difference is created across the superleak. At a temperature below the λ-temperature of the mixture, this osmotic pressure difference gives rise to a superflow of ^{4}He from the lower vessel to the upper vessel because the superleak acts as a semi-permeable membrane; the creeping film along the glass capillary provides the contact between the bulk liquid in A and the superleak. Since the transfer capacity of the superleak is very large the transfer rate is determined by the film and can be measured from the lowering of the liquid level in A.

The flow of ^{4}He from A to B, however, gives rise to an increase of the ^{3}He concentration in A and a corresponding decrease of the ^{3}He concentration in B. As a result the osmotic pressure difference decreases and the process tends to an equilibrium. The final equilibrium state, however, depends on the quantities and concentrations of the mixtures initially present in A and B. First, it is possible that the bulk liquid in B comes into equilibrium with the remaining bulk liquid in A. In this case the concentration in B is nearly equal to the concentration in A; only a small osmotic pressure difference is required to maintain the difference in height of the liquid levels in A and B. Secondly, there may still be a concentration difference after all the liquid has been removed from A. In this case the liquid in B exerts a tension on the film in A, equal to the remaining osmotic pressure difference. The film now becomes unsaturated and the pressure of the vapour in equilibrium with the film decreases below the saturated vapour pressure.

After equilibrium has been reached a new run is easily performed. When a small quantity of ^{3}He is added to vessel A, a flow of ^{4}He in the opposite direction takes place and vessel A is filled again. Simultaneously the concentration has been increased. On the other hand the concentration can also be decreased by pumping off some vapour in B and A respectively.

During the measurements the level of the surrounding helium bath was always above the upper vessel B and the temperature of the bath was monitored within 10^{-4} °K. A cotton wick, wrapped around the capillaries C and D up to about 20 cm above vessel B, reduced the heat leak from the top of the cryostat to the lower part of the apparatus when the bath level

was low. This helped to avoid a temperature difference between bath and apparatus.

The height of the liquid level in A was measured as a function of time. From the readings on the oil manometer and the bath pressure the vapour pressures in A and B were known as a function of time; the liquid concentration was deduced from the vapour pressure. During various checks no influence of the light on the transfer rate was found. Measurements were made with three glass capillaries of different size, to which we shall refer as capillary I, II and III; capilary I: length 10 cm, diameter 0.056 cm; capillary II: length 10 cm, diameter 0.158 cm; capillary III: length 2.6 cm, diameter 0.158 cm. Capillary I was a prism capillary of the type used for mercury thermometers. Capillary III was obtained by melting off the lower part of capillary II.

In order to obtain the transfer rate of the film from the lowering of the liquid level in A a few corrections have to be applied. These corrections appear as follows. The total molar content of vessel A is given by:

$$N = V_l \rho_l + V_v \rho_v$$

where V_l and V_v denote the volume of the liquid and of the vapour respectively and ρ_l and ρ_v the corresponding molar densities. If the number of moles ^{4}He which move to vessel B per unit time by film flow is given by $\dot{N}_f$, we may write:

$$\dot{N}_f = -\dot{N} = -\dot{V}_l(\rho_l - \rho_v) - V_l\dot{\rho}_l - V_v\dot{\rho}_v. \qquad (2)$$

The last two terms are small compared to the term with $\dot{V}_l$. They yield corrections for the change in density of liquid and vapour due to the change of the concentration. At low temperatures, however, these corrections together may amount to about 10%.

Eq. (2) holds only if no ^{3}He leaks through the superleak. This condition may easily be checked in two different ways:

1) The ^{3}He leak in vessel A during the run can be calculated from

$$\dot{N}_3 = \frac{d}{dt}(V_l \rho_l X_l + V_v \rho_v X_v) \qquad (3)$$

where X_l and X_v are respectively the liquid and the vapour concentration.

2) When all the liquid has been removed from A and a concentration difference and hence a pressure difference still acts across the superleak, the pressure increase in vessel A can be observed. This pressure increase is a measure of the ^{3}He leak, for the partial pressure of the ^{4}He in the lower vessel remains nearly constant when only gas is present in A. The ^{3}He leak was found to be smaller than 2% of the observed flow rates.

3. *Measurements and results.* The first measurements were made with capillary I. In this case the smallest constriction which determines the film

flow is the perimeter of the capillary itself. The choice of these dimensions of the capillary had been made because the small cross-section provided the possibility of measuring the small transfer rates, as had been observed by Wansink and Taconis. But the first results showed already that the transfer rates exceeded the expected values considerably. To get reliable runs, of ten minutes or more, it was therefore necessary to start with a relatively large quantity of liquid in A (20–25 mm^3), except at temperatures in the vicinity of the λ-temperature. Fig. 2*a* shows a few typical results at the temperature 1.73°K. In this graph the change of the level height per unit time $\dot{H}$ has been plotted against the liquid concentration in A for four separate runs. From the graph it is clear that the slope of the curves is not determined by the concentration only. There are, however, two possible effects which could influence the slopes. The most likely is a dependence of the film flow on film height or path length. The determining parameter in this case would be the distance H from the liquid level to the upper end of the capillary (fig. 1). The path length varied appreciably during a run, as is demonstrated by the numbers attached to the curves which indicate the initial and final path length in mm. A second cause is indicated by the results of Wansink

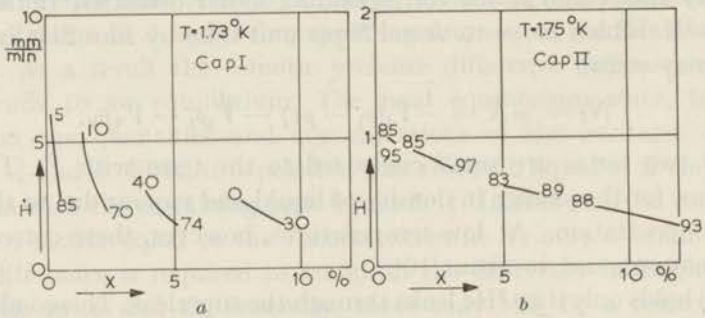

Fig. 2. The change of the level height per unit time $\dot{H}$ as a function of the liquid concentration in the lower vessel X for four separate runs. The numbers at the curves indicate the initial and final path length. *a*) capillary I *b*) capillary II.

and Taconis, for these authors found a slight dependence of the transfer rate on pressure head. The pressure head is in this case the osmotic pressure difference and it also varied appreciably during a run. It is evident that under these experimental conditions it is not possible to separate the two effects in a simple and rigourous way. Therefore, only a few measurements were made with this capillary. However, from the results of different days it became also clear that the reproducibility was insufficient. We concluded that this was due to impurities; we indeed found that, also for mixtures with high ^{3}He concentration impurities cause a strong increase of the film transfer rate. Up to this point in the experiments the mixtures had been led over charcoal at liquid air temperature before the measurements. From this time on, the purification was improved by leading the gaseous mixtures

through a coil in an apart cryostat with liquid helium at the normal boiling point. At the same time capillary I was replaced by capillary II. Fig. 2*b* represents four typical runs with capillary II. Because the diameter of capillary II is about three times as large as the diameter of capillary I the change of height of the liquid level per unit time and thus the change of path length during a run is considerably smaller. Usually a quantiy of 30–40 mm³ of liquid mixture was condensed in A; thus the average liquid level was about 10 mm from the bottom of the capillary. In fact the change of height now was negligibly small compared to the full length of the capillary. This may be seen from the numbers attached to the curves which indicate, as in fig. 2*a*, the initial and final path length. The separate curves in fig. 2*b* lie nearly on one curve. Since the variation of pressure head for these runs is of the same order of magnitude as for the runs represented in fig. 2*a*, we conclude that the effect of pressure head is small. Furthermore, at equal height and concentration the value of $\dot{H}$ differs by about a factor of three for the two capillaries. Therefore we are also tempted to conclude that the flow rate is proportional to the perimeter of the capillary; as the diameter of capillary I is 0.56 mm and the diameter of capillary II 1.58 mm. However, as mentioned in section 2, there is a constriction of about 1.2 mm diameter in the brass cap of the superleak; and the question arises whether indeed the glass capillary is the constriction determining the film flow. In this connection it may be emphasized that no special precautions had been made to obtain a smooth inner surface of the bore in the cap. After a study of the effect of surface finish on film transfer, Smith and Boorse[8]) report, for nickel *e.g.*, a difference of 60% between the flow rate over a finished and an unfinished surface. For this reason it seems quite plausible to us that in our apparatus with capillary II the perimeter of the glass capillary is still the constriction determining the film flow.

In order to examine the question as to whether indeed the effect of pressure head is observable or not, a number of runs were measured at 1.598°K, at various pressure heads. The results are shown in fig. 3. Only

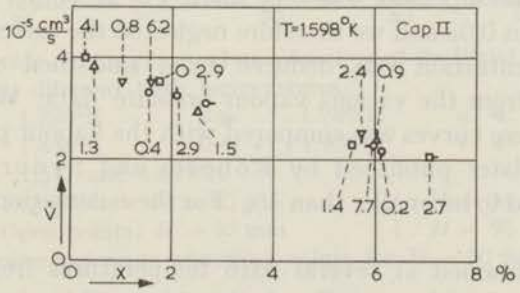

Fig. 3. The flow rate $\dot{V} = \dot{N}/\bar{V}_4{}^0$ in capillary II at a path length of 85 mm as a function of the liquid concentration in the lower vessel X. The numbers at the points indicate the concentration differences ΔX in % between upper and lower vessel.

transfer rates corresponding with a path length of 85 mm have been selected. The concentration differences determining the osmotic pressure head are indicated in the graph. We note that the osmotic pressure difference at this temperature is about 300 cm helium per percent concentration difference, hence the pressure head varies from 0 to 2000 cm helium. Since the points in fig. 3 are randomly scattered, the influence of pressure head must be very small in the considered range. Also, at other temperatures we found no indications for an effect of pressure head. In this connection we must remark, however, that a pressure dependence may exist in the range of very small pressure heads of 5 or 10 cm helium. We cannot give an opinion about the behaviour in that range because this is very near to equilibrium in our experiment and several spurious effects may occur when the equilibrium level is closely approached. In any case our results do not depend on the concentration in the upper vessel, and this behaviour yields an indication that in our case the flow is completely determined by the properties of the film in the lower vessel.

In a run where final equilibrium is reached while liquid is still present in A the leak of ^{3}He is very small near to the equilibrium state because the pressure difference across the superleak then becomes very small. Near to equilibrium we may therefore apply eq. (3) with $\dot{N}_3 = 0$. Eq. (3) then reduces to:

$$\frac{\mathrm{d}}{\mathrm{d}t}(V_\mathrm{l}\rho_\mathrm{l}X_\mathrm{l} + V_\mathrm{v}\rho_\mathrm{v}X_\mathrm{v}) = 0.$$

Using this equation, the vapour volume V_v can be calculated. We found V_v nearly equal to the low temperature part of the actual vapour volume. The creeping film in capillary D evidently supplied enough ^{4}He in the high temperature part of the vapour volume to build up the required pressure increase. This was taken into account in the calculation of the vapour correction according to eq. (2). The correction due to the change of liquid density was calculated from the data of Kerr [9]) on the density of liquid mixtures. The leak tests, as mentioned in section 2, showed that the leak of ^{3}He through the superleak was very small. For all points $\dot{N}_3/\dot{N}$ was found to be smaller than 0.02 and we therefore neglected the correction due to this leak. The concentration was deduced from smoothed vapour pressure curves, derived from the various vapour pressure data. When the vapour pressure from these curves was compared with the vapour pressure deduced from the table later published by Roberts and Sydoriak [10]), the deviations appeared to be smaller than 1%. For these deviations no corrections were made.

The results obtained at several bath temperatures from 1.3 to 2.1°K are shown in fig. 4. In this graph $\dot{N}$, calculated from (2) has been plotted *versus* concentration. Only points corresponding to distinct path lengths have been selected. Those path lengths have been chosen which are covered by most

runs: $H = 93$ mm and $H = 90$ mm. The drawn curves in the graph are smoothed curves corresponding to a path length of 90 mm.

In order to investigate the effect of path length we could have made measurements with a large quantity of liquid in capillary II. It is, however, more practical to operate with a small quantity of liquid and therefore the capillary was made shorter by melting off a part of it. The separate curves, representing the various runs at constant temperature obtained with capillary III were not found to lie on one curve in this case, because the relative change of path length during a run was now larger. The transfer

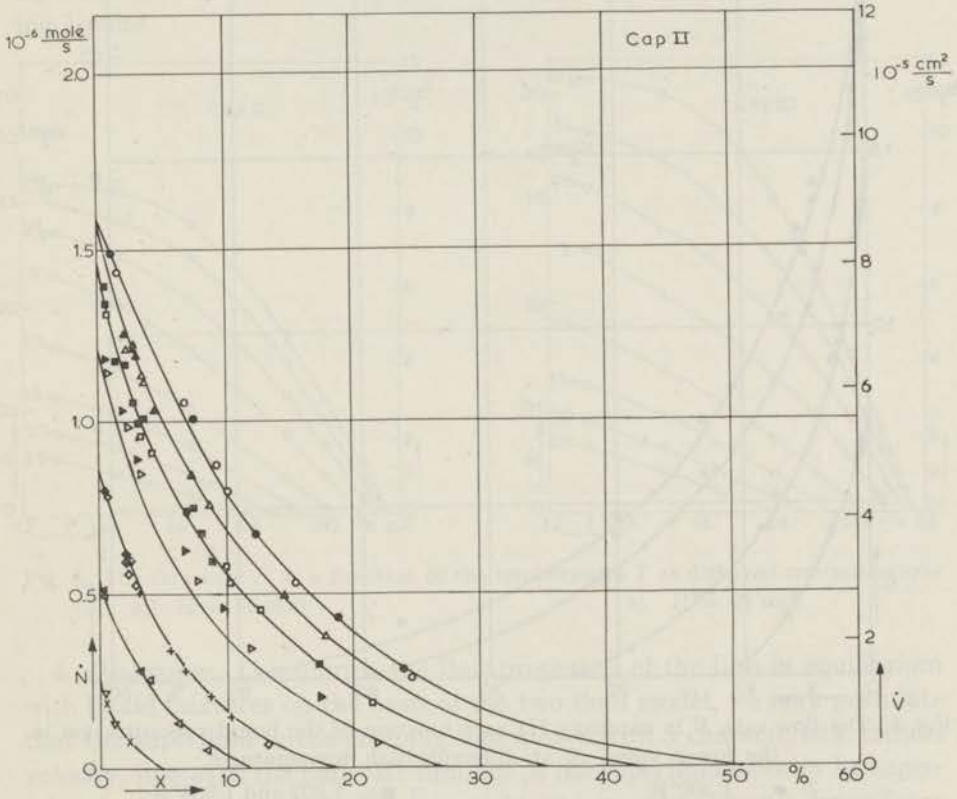

Fig. 4. The flow rate $\dot{N}$ in capillary II as a function of the liquid concentration in the lower vessel X at different bath temperatures.

○ ●: 1.288°K ▷ ▶ : 1.749°K ◁ ◀: 1.996°K
△ ▲: 1.450°K ◇ ◆ +: 1.900°K ▽ ×: 2.101°K
□ ■: 1.597 and 1.599°K
Full points: $H = 90$ mm × : $H = 94$ mm
Open points: $H = 93$ mm + : $H = 95$ mm
The curves drawn represent smoothed values for $H = 90$ mm.

rates at path lengths of 19 mm and 21 mm were selected. The results are shown in fig. 5. The drawn curves are smoothed curves corresponding to a

path length of 21 mm. Figs. 6*a* and 6*b* show the transfer rates with capillaries II and III respectively as a function of temperature at distinct concentrations. The points plotted in these graphs correspond to intersections with the curves of the figs. 4 and 5. For a comparison we added a cm^2/s scale, differing from the mole/s scale by a factor $\overline{V}_4{}^0/p = 27.45/p$ cm^2/mole, where $\overline{V}_4{}^0$ is equal to the mean molar volume of liquid ^4He in the temperature range considered and p is the perimeter of the capillary. The relation between the quantities $\dot{V}$

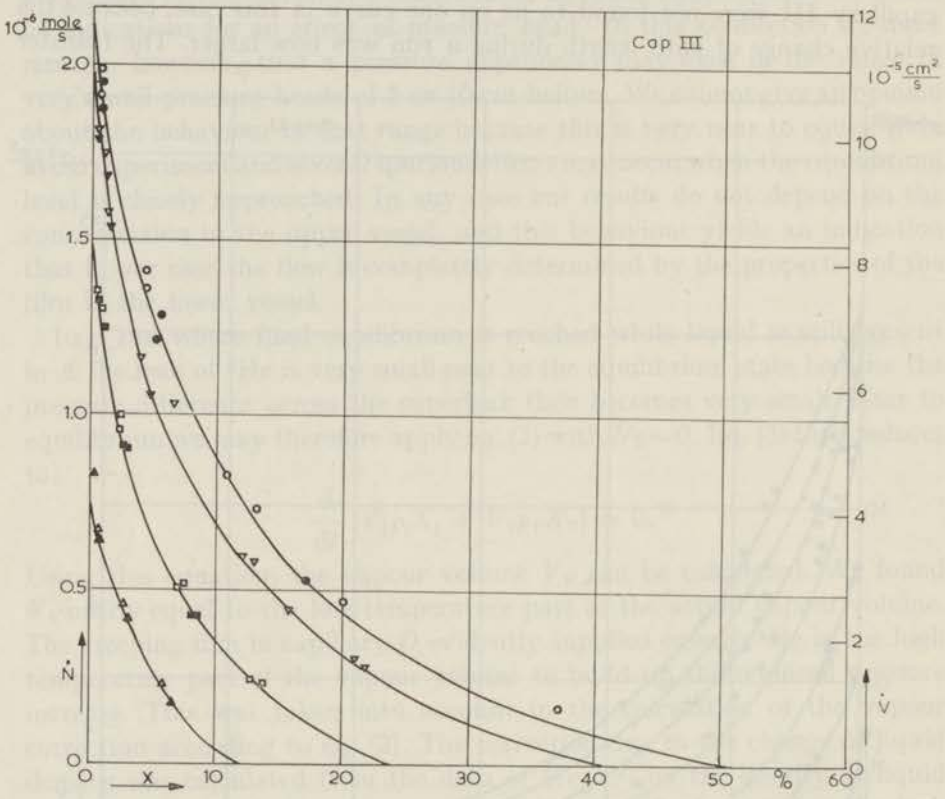

Fig. 5. The flow rate $\dot{N}$ in capillary III as a function of the liquid concentration in the lower vessel X at different bath temperatures.

○ ●: 1.300°K □ ■: 1.802 and 1.804°K
▽ ▼: 1.495 and 1.501°K △ ▲: 2.000°K
Full points: $H = 21$ mm Open points: $H = 19$ mm
The curves drawn represent smoothed values for $H = 21$ mm.

(indicated on the right hand side in the figs. 4 and 5), σ (as defined by formula (1)) and $\dot{N}$ is given by:

$$\dot{N} = \dot{V}p/\overline{V}_4{}^0 = \sigma p/V_1.$$

The deviations of $V_4{}^0$ from $\overline{V}_0{}^4$ are smaller than 0.5%, and for $X = 0.25$ the largest deviation of V_1 from $\overline{V}_4{}^0$ is 8%.

The flow rates of pure ^{4}He, as found after extrapolating the curves of figs. 4 and 5 to zero concentration, agree fairly well with the transfer rates which have been found by others on clean glass surfaces. We may refer to the review of Smith and Boorse [8]) from which we see that ,depending on the height of the film and the sort of glass, values have been found varying between 7–13 cm^2/s at temperatures between 1.0 and 1.5°K. In this temperature range we found for capillary II about 8 cm^2/s and for capillary III about 12 cm^2/s (fig. 6).

The flow rate decreases very rapidly when ^{3}He is added and the results indicate that the curves extrapolate to zero transfer rate at the corresponding λ-point.

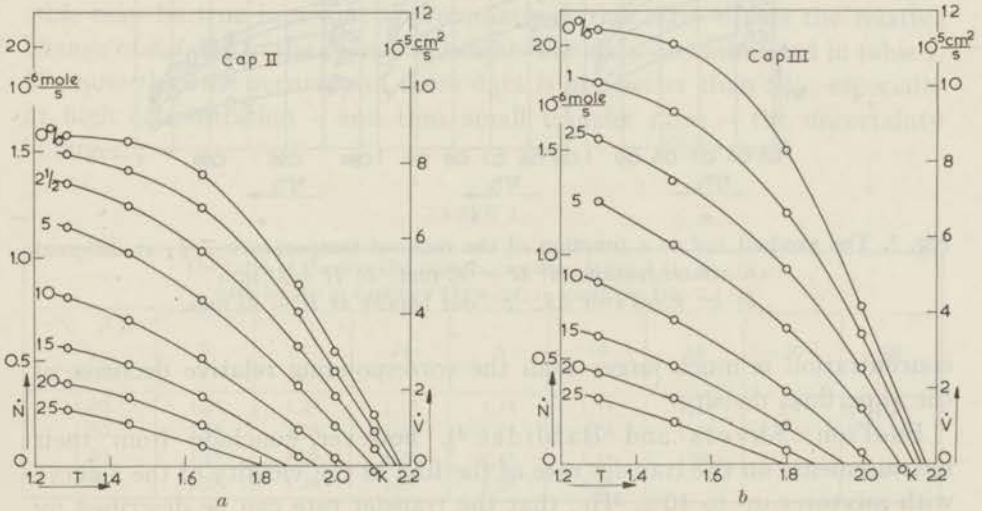

Fig. 6. The flow rate $\dot{N}$ as a function of the temperature T at different concentrations
a) $H = 90$ mm *b*) $H = 21$ mm.

4. *Discussion.* Considering the flow properties of the film in equilibrium with liquid mixtures on the basis of the two fluid model, we may postulate that the superfluid in the creeping film moves with a characteristic critical velocity, just as in the pure ^{4}He film, for ,if the superfluid velocity be supercritical, a mutual friction will occur, and in this case we expect a dependence of the flow rate on pressure head. Such a dependence, however, has not been observed; hence we may assume the superfluid velocity to be completely determined by the properties of the film itself.

If it is further assumed that the superfluid density in the film is equal to the superfluid density in the bulk liquid the value of $v_c d$ can be calculated from our results according to formula (1). Andronikashvili's type of experiment for determining ρ_n in bulk liquid mixtures has been performed by Berezniak and Esel'son [11]) and by Dash and Taylor [12]). Due to a discrepancy between these data there is some uncertainty in the value of

ρ_n. We used the values as obtained by Dash and Taylor. In fig. 7*a* we plotted $v_c d$ as deduced from the transfer rates in capillary II against the reduced temperature T/T_λ at distinct concentrations. Fig. 7*b* shows the similar curves from the transfer rates in capillary III. These graphs exhibit a variation of more than a factor 2 in the value of $v_c d$. Such a variation cannot be explained by the uncertainty in the values of ρ_s. As a result we may conclude that the relative decrease of the flow rate with increasing

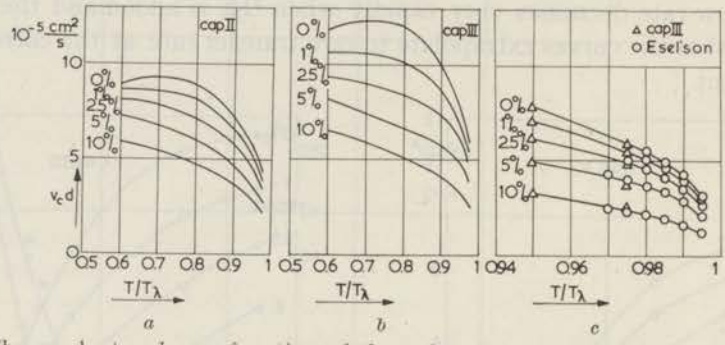

Fig. 7. The product $v_c d$ as a function of the reduced temperature T/T_λ at different concentrations *a*) $H = 90$ mm *b*) $H = 21$ mm *c*) ○: Esel'son *e.a.* △: our results at $H = 21$ mm.

concentration is much larger than the corresponding relative decrease of the superfluid density.

Esel'son, Shvets and Bablidze [4]), however, conclude from their measurements on the transfer rate of the film in the vicinity of the λ-curve with mixtures up to 10% ^{3}He, that the transfer rate can be described by the simple formula:

$$\sigma = A\rho_s/\rho \qquad (4)$$

where A is a constant, equal to 3.2×10^{-5} cm^2/s. According to formula (1) A is equal to $v_c d$.

Evidently, formula (4) with constant A cannot give an adequate description of the transfer rate as a function of temperature and concentration in a wide range below the λ-curve. For pure ^{4}He and $\rho_s/\rho \approx 1$ eq. (4) with $A = 3.2 \times 10^{-5}$ cm^2/s yields a value for σ which is too small by more than a factor 2. Therefore we recalculated $v_c d$ from the data of Esel'son *e.a.* These values of $v_c d$, which are also far from constant, are plotted in fig. 7*c* together with some values of $v_c d$ as obtained from the flow rates in capillary III. We note that the choice of ρ_s-values does not influence the results because the differences between the data of Dash and Taylor and the data of Berezniak and Esel'son are very small near the λ-curve. As we do not know the path length of the film in the apparatus of Esel'son *e.a.* we may only compare the dependence on temperature and concentration.

This dependence appears to be the same in both experiments. We may conclude, therefore, that formula (4), with constant A, cannot describe the transfer rate adequately, even in the small temperature range investigated by the Russian authors.

If the superfluid velocity in the film is determined by the conditions in the film, the variation of the flow rate with the path length is only due to the variation of the film thickness with the height above the liquid level, *i.e.* the film profile. As the conditions in capillary II and III only differ by the difference in path length of the film we may consider the ratio of the transfer rates in the two capillaries in order to discuss the effect of film height. If we assume the superfluid density in the film to be independent of height (this may be true in a first approximation), this ratio equals the relative change of $v_c d$ due to the change of height. The data are tabulated in table I. We note that the accuracy of these data is not better than 5%; especially at high concentration – and thus small transfer rates – the uncertainty is larger.

TABLE I

The ratio of the transfer rates in capillary III and II: $\dot{N}_{III}/\dot{N}_{II}$; path length in capillary II: 9 cm; in capillary III: 2.1 cm

T°K \ X%	0	1	2½	5	10	15	20	25
1.30	1.30	1.25	1.15	1.10	1.10	1.10	1.10	1.20
1.50	1.30	1.25	1.15	1.10	1.05	1.05	1.05	1.15
1.80	1.35	1.25	1.20	1.15	1.10	1.05		
2.00	1.35	1.35	1.35	1.35	1.30			

As a consequence of the decrease of film thickness with increasing height the flow rate obviously decreases. This implies that the relative decrease of film thickness exceeds the corresponding relative increase of superfluid velocity. Hence, the flow rate is in any case determined by the film thickness at the upper end of the smallest constriction above the liquid level.

At zero concentration the variation of the flow rate with height is nearly temperature independent. This result is consistent with the data on the thickness of the pure ^{4}He film [13]) which have been found to vary only slightly with temperature in the temperature range considered. In accordance with this behaviour the transfer rate of a film of pure ^{4}He may be described by a formula of the form $\sigma = \alpha(T)\,\beta(H)$. For β the expression $H^{-1/z}$ is often used, based on the relations: $v_c \sim d^{1/z_1}$ and $d \sim H^{-1/z_2}$. Presumably, however, the relation between d and H is more complicated [14]). Moreover, according to Smith and Boorse [8]), the function $H^{-1/z}$ for β is too simple for an adequate description of the observed dependence of the flow rate on height. We found a relative increase of the flow rate of 30% corresponding

to a change of height from 9 to 2 cm. A similar increase of the flow rate of the pure ^{4}He film with decreasing height has been observed by Smith and Boorse [8]).

In general, for mixtures d will be a function of temperature, concentration and height and v_c a function of temperature, concentration and d. It is therefore not surprising that the dependence of transfer rate on height is complicated in the case of mixtures, This is clearly shown by table I. The variation with height seems to depend on both temperature and concentration. In view of these results one may wonder, however, whether the constriction determining the film flow is the same for all the measurements. As we mentioned in section 2 there are two constrictions in our apparatus: the capillary itself and the bore in the cap of the superleak, and we assume that the capillary constriction determines the flow. If, however, during a run a change should occur such that the bore in the cap would determine the flow this would give rise to a discontinuity in the second derivative of the curve h *versus* time, which is of course hardly detectable. The scatter of the points in the graph $\dot{N}$ *versus* X (figs. 4 and 5), on the other hand, makes it also difficult to ascertain whether a discontinuity in the slope of these curves is present. With capillary II a change of constriction, however, is very unlikely, because the difference in height of the two constrictions is relatively small in this case; but with capillary III this is questionable. Since data on the thickness of the film in equilibrium with a liquid mixture are lacking further analysis of the height dependence must be postponed.

As we pointed out before, in the special case when all the bulk liquid has been removed from the lower vessel, the film becomes unsaturated under the influence of the remaining osmotic pressure head. The decrease of the pressure below the saturated vapour pressure is related to the concentration difference between upper and lower vessel from which this pressure decrease originates. The similar behaviour of the film of pure ^{4}He under the influence of a fountain pressure was already investigated in an earlier experiment [15]). As in that case the decrease of pressure is related to the fountain pressure, the method was used for indirect measurements of the fountain effect. The relation between the pressure decrease Δp and the employed fountain pressure head π_f was shown to be:

$$\Delta p = \frac{\bar{\rho}_v}{\rho_l} \pi_f \qquad (5)$$

where $\bar{\rho}_v$ is the mean density of the vapour in the range of the pressure variation Δp and ρ_l the bulk liquid density.

Now, we have mixtures of different concentration in the two vessels whereas the temperature is homogeneous throughout the system. The relation between the pressure decrease Δp and the osmotic pressure head π_{osm} now can directly be derived from the conditions of osmotic equilibrium.

As a matter of fact, Δp is equal to the difference between the partial vapour pressure of ^{4}He in the last drop of liquid in the lower vessel, $p_4(X_1)$, and the final partial pressure of ^{4}He of the gas in the lower vessel, after equilibrium has been reached, p_4^f. From the equality of the partial chemical potentials of the ^{4}He in the upper and the lower vessel it follows that p_4^f equals $p_4(X_2)$, the partial vapour pressure of ^{4}He in the upper vessel. As π_{osm} is related to $p_4(X_1)$ and $p_4(X_2)$ by the equation:

$$\pi_{osm} = \frac{RT}{V_4} \ln \left[\frac{p_4(X_1)}{p_4(X_2)} \right]$$

we find

$$\Delta p = p_4(X_1) \left[1 - \exp\left(- \frac{V_4}{RT} \pi_{osm} \right) \right] = \bar{\rho}_{4,v} V_4 \pi_{osm}$$

where V_4 is the partial molar volume of ^{4}He in the liquid and $\bar{\rho}_{4,v}$ is the mean vapour density of the ^{4}He in the range of pressure variation Δp. Below the λ-temperature, V_4 is nearly independent of concentration and equal to V_4^0, the molar volume of pure ^{4}He. Quite analogous to eq. (5) we may therefore write:

$$\Delta p = \frac{\bar{\rho}_{4,v}}{\rho_{4,l}} \pi_{osm}. \qquad (6)$$

Unfortunately, however, we could not derive the pressure decrease with sufficient accuracy from our observations. This may be illustrated by fig. 8.

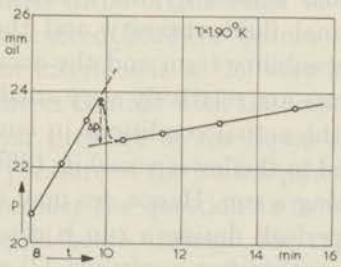

Fig. 8. A typical example of the observed pressure change in the lower vessel, as it is emptied; p is the difference between vapour pressure and bath pressure.

In this graph, the vapour pressure in the lower vessel has been plotted *versus* time for a typical run. The curve was obtained from two curves corresponding to the readings on two levels of the oil manometer. In general our observations appeared to be inadequate for an accurate construction of the curve in the interval of pressure decrease. But even if it had been possible to construct the curve the slowness of the adjustment of the oil levels could have influenced the results, because the pressure decreases in a relatively small time interval. In spite of these difficulties we can

establish that the observed pressure drops agree in order of magnitude with formula (6).

5. *Some reflections on the flow phenomena in the superleak.* In order to ascertain whether slit effects did not influence the observed transfer rates we are led to consider in detail the conditions in the superleak. When discussing the flow properties in the superleak on the basis of the two fluid model we may assume the normal fluid to obey Poiseuille's law, whereas the superfluid flows without friction, provided the velocity is small. As soon as the superfluid velocity, however, surpasses a critical value a mutual friction arises between the two fluids. The equations of motion originally proposed by Gorter and Mellink for pure ^{4}He, are later, in extended form, found to be also applicable to the case of mixtures. Mazur [16]) *e.g.*, derived two equations of motion on the basis of irreversible thermodynamics, one equation for the superfluid and the other for the normal fluid including the ^{3}He. For the motion in a narrow slit in a stationary state and in the absence of mutual friction these equations may be written:

$$-\frac{\rho_s}{\rho}\operatorname{grad} P + \frac{\rho_s}{\rho}\operatorname{grad} P_f + \frac{\rho_s}{\rho}\operatorname{grad} P_{osm} = 0 \tag{7}$$

$$-\frac{\rho_n}{\rho}\operatorname{grad} P - \frac{\rho_s}{\rho}\operatorname{grad} P_f - \frac{\rho_s}{\rho}\operatorname{grad} P_{osm} + \eta_n \nabla^2 v_n = 0 \tag{8}$$

where P denotes the "mechanical" pressure (hydrostatic pressure, vapour pressure *etc.*), P_f the fountain pressure caused by the temperature gradient, P_{osm} the osmotic pressure caused by the gradient of ^{3}He concentration, and η_n and v_n the normal fluid viscosity and the normal fluid velocity respectively. The compressibility term and the acceleration terms are neglected because these terms are relatively very small.

Let us now consider the actual conditions in our experiment. We found that when ^{3}He was added to the lower vessel its filling rate greatly exceeded its rate of emptying during a run. Hence, we may conclude that the superfluid velocity in the superleak during a run is considerably lower than its critical value, and we may therefore apply eqs. (7) and (8). Furthermore the whole apparatus is surrounded by a constant temperature bath. We may consequently presume that the temperature difference across the superleak must be very small, if it exists at all. The second term on the left hand side in the eqs. (7) and (8) is in any case small compared with the third term which originates from the concentration difference. We may therefore omit the second term, and eqs. (7) and (8) now become:

$$\frac{\rho_s}{\rho}\operatorname{grad} P = \frac{\rho_s}{\rho}\operatorname{grad} P_{osm} \tag{9}$$

$$\frac{\rho_n}{\rho}\operatorname{grad} P + \frac{\rho_s}{\rho}\operatorname{grad} P_{osm} = \eta_n \nabla^2 v_n. \tag{10}$$

Since the normal fluid containing the ^{3}He flows from the upper vessel to the lower vessel, the concentration in the superleak will mainly be governed by the concentration in the upper vessel, the concentration gradient being limited to the lower end of the superleak. After substitiuton of eq. (9) into eq. (10) and integration over the slit length, we arrive at the equations:

$$\Delta P = \Delta P_{\mathrm{osm}} \tag{11}$$

$$\Delta P = C\eta_{\mathrm{n}}\bar{v}_{\mathrm{n}} \tag{12}$$

where $\bar{v}_{\mathrm{n}}$ is the mean normal fluid velocity in the superleak and η_{n} the viscosity of the normal fluid, which is roughly equal to the viscosity of the mixture in the upper vessel. C is a constant, determined from the size, shape and distribution of the channels. According to eq. (11) the osmotic pressure head must be balanced by a mechanical pressure head. The osmotic pressure head may vary from zero to several thousand cm helium, depending on the quantities of liquid and their concentrations, initially present in the vessels. The hydrostatic pressure head and the vapour pressure difference are small compared to ΔP_{osm}. The largest part of ΔP_{osm} must therefore be balanced by the surface tension of the liquid vapour interface at the lower end of the superleak. Making a rough estimate of the surface tension exerted at the interface when the radius of curvature is equal to half the diameter of the channels in the superleak we find a pressure of some 10^3 cm helium. (From measurements with an electron microscope, the diameter of the grains of the powder appeared to be about 3×10^{-6} cm. Hence the size of the channels can be estimated to be of the order of 10^{-6} cm). If the osmotic pressure head does not exceed 2000 cm helium – as is the case in most runs – the liquid vapour interface is at the very low end of the superleak; the interface being in direct contact with the vapour of the mixture in the lower vessel. The vapour pressure of the liquid at the interface thus will be equal to the vapour pressure of the bulk liquid in the lower vessel.

Now we shall first consider the question as to whether a transport takes place from the bulk liquid below through the vapour to the superleak or conversely. According to eqs (11) and (12) the pressure head acting on the normal fluid equals ΔP_{osm}. The normal fluid consists of ^{3}He and normal ^{4}He. The ^{3}He coming down through the superleak must evaporate at the lower end, as the equilibrium vapour pressure must be maintained. The normal ^{4}He, however, being at the lower end of the superleak, may become superfluid and return with the superfluid flow upwards. To a first approximation we may assume the heat exchange with the surrounding bath to be negligibly small, since the heat conductivity of the powder is extremely bad. The heat balance at the lower end of the superleak is then expressed by the equation:

$$\bar{v}_{\mathrm{n}}\rho O_{\mathrm{e}}\{XL_3 - xTS_4 - \delta(L_4 + TS_4)\} = 0. \tag{13}$$

O_e is the effective cross section of the superleak. X is the ^{3}He concentration and x the fraction normal ^{4}He in the superleak; both quantities being mainly determined by the mixture in the upper vessel. L_3 and L_4 denote the partial molar heat of evaporation of ^{3}He and ^{4}He respectively under the actual conditions, and S_4 the partial molar entropy of liquid ^{4}He. δ indicates the fraction ^{4}He which condenses or evaporates; δ is positive when $XL_3 > > xTS_4$ and condensation occurs; δ is negative when $XL_3 < xTS_4$ and evaporation occurs. At high concentrations or high temperatures the evaporation of ^{3}He is mainly balanced by conversion of normal ^{4}He into superfluid ^{4}He; thus δ is relatively small in that case. But, apart from this, we can conclude from eq. (13), that δ is smaller than X, because $L_4 > L_3$. Since we experimentally found $\bar{v}_n \rho O_e X$ (*i.e.* the ^{3}He leak through the superleak) to be small compared to the flow rate of the film (smaller than 2% of it), and since $\bar{v}_n \rho O_e \delta$ is smaller than $\bar{v}_n \rho O_e X$, we conclude that condensation or evaporation at the lower end of the superleak does not seriously influence the flow rate in our experiment.

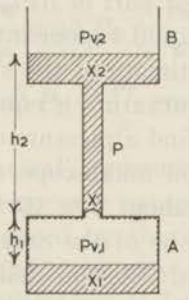

Fig. 9. Schematic diagram illustrating the conditions in a pore P of the superleak.

We may also consider the osmotic equilibrium more accurately. We assume the temperature constant throughout the whole system. A diagram of the situation is given in fig. 9, where P schematically represents a pore in the superleak.

X_1 denotes the ^{3}He concentration of the liquid in the lower vessel and $p_{v,1}$ the corresponding vapour pressure. The similar quantities for the upper vessel are X_2 and $p_{v,2}$. The length of the liquid column in the upper vessel, including the superleak, is h_2. According to eqs. (11) and (12) is:

$$\Delta P_{osm} = \Delta p_v + h_2 \rho_{l,2} + \Delta P_{surf} = \Delta P_{surf} + \Delta P_{cor} \qquad (14)$$

where ΔP_{osm} is the osmotic pressure difference across the superleak, ΔP_{surf} the surface tension of the curved interface at the lower end of the superleak, $\Delta p_v = p_{v,2} - p_{v,1}$ and $\rho_{l,2}$ the density of the liquid in the upper vessel.

Due to the curvature of the interface at the lower end of the superleak, the internal pressure of the liquid is decreased, the pressure decrease being

equal to ΔP_{surf}. The internal pressure of the liquid at the curved interface therefore is different from the internal pressure of the liquid at the planar interface in the lower vessel. Since the vapour pressure depends on the internal pressure of the liquid, but the total vapour pressure is homogeneous throughout the vessel – for the sake of simplicity we neglect the effect of gravity in the film and the vapour of the lower vessel – the concentration of the liquid at the two interfaces must be different. Denoting the concentration in the liquid at the curved interface by X, and the internal pressure by $P - \Delta P_{surf}$, the second condition, with respect to the vapour pressure in equilibrium with the liquid behind the curved interface, may be written:

$$p_v(X, P - \Delta P_{surf}) = p_3(X, P - \Delta P_{surf}) + p_4(X, P - \Delta P_{surf}) = p_{v,1} \quad (15)$$

where p_3 and p_4 are the partial vapour pressures of ^{3}He and ^{4}He respectively.

The equation for the osmotic pressure difference in the liquid finally is:

$$\Delta P_{osm} = \frac{RT}{V_4} \ln \left[\frac{p_4(X, P - \Delta P_{surf})}{p_4(X_2, P - \Delta P_{surf})} \right]. \quad (16)$$

V_4, the partial molar volume of ^{4}He in the liquid, is nearly independent of X below the lambda curve, and equal to V_4^0, the molar volume of pure ^{4}He. Applying the thermodynamic relations:

$$\ln \left[\frac{p_3(X,P)}{p_3(X, P - \Delta P_{surf})} \right] = \frac{V_3}{RT} \Delta P_{surf} \text{ and}$$

$$\ln \left[\frac{p_4(X,P)}{p_4(X, P - \Delta P_{surf})} \right] = \frac{V_4}{RT} \Delta P_{surf}$$

the eqs. (14), (15) and (16) lead to:

$$\frac{p_3(X)}{\{p_4(X)\}^{V_3/V_4}} = \frac{p_{v,1} - p_4(X_2) \exp(\Delta P_{cor} V_4/RT)}{\{p_4(X_2)\}^{V_3/V_4} \exp(\Delta P_{cor} V_3/RT)}.$$

In the last equation all vapour pressures relate to the internal pressure P. This parameter has for the present been omitted. Because $\Delta P_{cor} V_4 \ll RT$ the equation can be simplified to:

$$\frac{p_3(X)}{\{p_4(X)\}^{V_3/V_4}} = \frac{p_3(X_2)}{\{p_4(X_2)\}^{V_3/V_4}} \left[1 - \frac{\Delta p_v}{p_3(X_2)} \right]. \quad (17)$$

Since V_3, just as V_4, is nearly independent of concentration below the lambda curve, the concentration X can be determined graphically from eq. (17), if the distribution coefficient be known. We performed this calculation for a special case. According to De Bruyn Ouboter, Beenakker and Taconis [17]) the vapour pressure of ^{3}He–^{4}He mixtures at low temperaturer can approximately be described by considering the mixture as a regular

TABLE II

The composition of the liquid (X) and the vapour ($C_v = p_3/p_4$) at the curved interface for fixed liquid concentration in upper and lower vessel (X_2 and X_1)

$T = 1.288°K$					$T = 1.599°K$				
X_1	X	X_2	$C_v(X_1)$	$C_v(X)$	X_1	X	X_2	$C_v(X_1)$	$C_v(X)$
0.0	0.0^6	5.0	0.0	0.0^4	0.0	0.1^5	5.0	0.0	0.0^5
5.0	5.3^7	10.0	3.6^8	3.8^8	5.0	5.4^8	10.0	1.4^3	1.5^2
10.0	10.7^0	15.0	6.9^0	7.2^5	10.0	10.8^5	15.0	2.7^4	2.9^2
15.0	16.0^0	20.0	9.7^5	10.1^5	15.0	16.1^2	20.0	3.9^6	4.1^8
20.0	21.2^5	25.0	12.2	12.7	20.0	21.4^3	25.0	5.0^9	5.3^5
25.0	26.6^0	30.0	14.5	15.0	25.0	26.7^4	30.0	6.1^6	6.4^6
30.0	31.8^5	35.0	16.5	17.1	30.0	32.0^4	35.0	7.1^9	7.5^5

solution with $W/R = 1.54°K$, where W is a characteristic constant of the regular solution. Assuming this to be true, we made the calculation at two different temperatures, for some fixed values of X_1 and X_2. The results are given in table II. The concentration behind the curved interface appears to be quite different from the concentration in the lower vessel. Hence, the effective osmotic pressure head acting on the liquid in the superleak is much smaller than the osmotic pressure head, calculated from the concentrations in upper and lower vessel (π_{osm}, introduced in section 4). Furthermore, the composition of the vapour in equilibrium with the curved interface $C_v(X) = p_3(X, P - \Delta P_{surf})/p_4(X, P - \Delta P_{surf})$ is slightly different from the composition of the vapour in equilibrium with the liquid in the lower vessel $C_v(X_1) = p_3(X_1, P)/p_4(X_1, P)$ (table II). This difference in composition gives rise to a small concentration gradient in the vapour near the interface. In connection with this we may remark that in our apparatus the distance between the superleak and the upper rim of the capillary is about 2 cm. It is therefore very unlikely that there is a concentration gradient in the capillary. The difference in composition could slightly influence, however, the pressure drop, which is observed when the liquid in the lower vessel has been removed, *i.e.* the shape of the curve of fig. 8, but this is outside of our accuracy.

As we already pointed out before, the surface tension balances for a great deal the osmotic pressure head. In a cylindrical channel the maximum surface tension is reached when the radius of curvature equals half the diameter of the channel. We may therefore wonder what happens when the concentration difference between upper and lower vessel is very large (*e.g.* larger than 10%). Because the channels in the powder leak are of irregular shape we are tempted to believe that at any concentration difference an interface can exist with the proper curvature. A limit may, however, be reached when the radius of curvature becomes of the order of film thickness. We tried to obtain an answer to this question from a comparison of the ^3He leak during

various runs. A few runs at 1.288°K had been made, starting with large concentration differences. $\dot{N}_3$ was calculated according to formula (3).

Assuming that the normal fluid obeys Poiseuille's law, $\dot{N}_3$ is proportional to $(X_2/V\eta_n)\,\Delta P_{osm}$, where V is the molar volume [9]) and η_n the normal viscosity [18]) of the liquid *). ΔP_{osm} was calculated according to formula (16), by means of eq. (17). A graph of $\dot{N}_3 V\eta_n/X_2$ versus ΔP_{osm} is shown in fig. 10. Although, in fact, the data do not meet the required accuracy, at low pressure heads they seem to fit the linear dependence. The slope of the line is roughly consistent with the estimated channel size. It is, however, not possible to draw a convincing conclusion for the behaviour at high pressure heads. The deviations from the straight line at large pressure heads possibly indicate an increase of the flow resistance. We remark, however, that the calculation of ΔP_{osm} may be wrong in this case. When the interface is drawn up into the superleak the flow becomes of a composite type, for one part of the length liquid flow, and for the other gas flow. The vapour pressure at the interface in the superleak then is higher than the vapour pressure in the lower vessel. Thus the value of ΔP_{osm}, derived by means of formula (17), is found too large in this case.

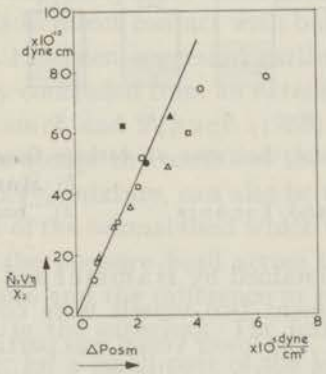

Fig. 10. The quantity $\dot{N}_3 V\eta/X_2$ as a function of the calculated pressure head $\Delta P = \Delta P_{osm}$ at the bath temperature 1.288°K. The various symbols indicate different runs.

Although it is not possible to estimate exactly the conditions and the resulting phenomena in and near the superleak, we believe to have enough evidence that the influence on transfer rate is very small. We should have expected a dependence of transfer rate on pressure head particularly if these phenomena influenced the results. But, as was shown in section 3, such a dependence has not been observed, at least not within the limits of accuracy

*) The effective viscosity is smaller than the bulk liquid viscosity if the mean free path for the ^{3}He in the mixture is of the order of the channel size. Presumably this is not the situation here, because for all points in fig. 10 $X \geqq 15\%$, except for the point marked ■, for which $X_2 = 6.5\%$.

6. *Some comments on the earlier flow measurements.* We will now return to the flow measurements already mentioned in the introduction. Daunt, Probst, Johnston, Aldrich and Nier [5]) made some measurements with a small Dewar vessel, closed at the top by a ground glass plug; the slit between the ground glass surfaces serving as a superleak. The Dewar vessel was partially immersed in a bath of atmospheric helium, containing $1.2 \times \times 10^{-4}\%$ ^{3}He, in such a way that the superleak was above the liquid level of the surrounding helium bath. A flow took place by means of the film along the outside wall of the vessel to the superleak and then into the vessel. The flow was maintained by supplying heat to the inside of the vessel. (The situation is schematically represented in fig. 11*a*). The liquid collected in the vessel was analyzed with a mass spectrometer and the ^{3}He fraction was found to be smaller than $5 \times 10^{-6}\%$. The transfer of ^{3}He through the slit therefore was relatively small compared to the transfer of ^{4}He.

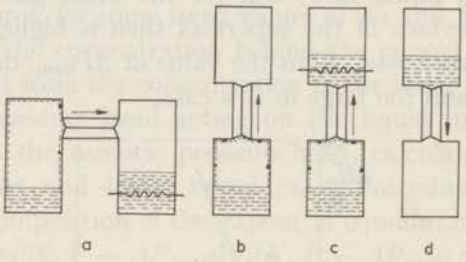

Fig. 11. Schematic diagrams of various flow experiments.
a) Daunt *e.a.* *b*) Hammel and Schuch
c) Wansink and Taconis *d*) "bulk liquid flow".

A similar result was obtained by Hammel and Schuch [6]) with a 3.9% mixture. In this experiment two vessels were connected by a platinum-in-pyrex glass superleak. The lower vessel was partially filled with the liquid mixture and the upper vessel was initially evacuated (fig. 11*b*). Observing the pressure in the upper vessel it was found that this rose rapidly until the partial vapour pressure of the ^{4}He in the lower mixture was reached and then slowly to the total vapour pressure. The flow rate of ^{3}He – which was independent of the gas pressure difference – was small compared to the flow rate of ^{4}He; the ratio varied from 0.03 at 1.57°K to 0.20 at 2.02°K.

In the experiment of Wansink and Taconis [7]) two vessels were connected by a gold-in-soft-glass superleak. The upper vessel contained pure ^{4}He and its temperature was raised until the fountain pressure exceeded the osmotic pressure of the mixture in the lower vessel. (fig. 11*c*). The flow rate was determined from the rise of the liquid level in the upper vessel. The transfer rate, as measured with a 1.3% mixture in the lower vessel, was much smaller than the transfer rate, as measured with pure ^{4}He; the difference was as much as a factor 10 at 2°K. As the observed transfer rate

with pure ^{4}He was nearly equal to the flow rate of the film over the smallest constriction near the entrance of the superleak, it was supposed that the film determined completely the transfer rate which had been measured with the mixture. No transfer of ^{3}He through the slit was observed during these measurements.

The experiment of Hammel and Schuch especially has been the source of suggestion that the ^{3}He may participate in the superfluid flow of the ^{4}He. However, this suggestion has never been confirmed in other experiments. Osborne, Abraham and Weinstock measured the flow rate of pure ^{3}He through a superleak into an evacuated volume. In this experiment the bulk liquid was in direct contact with the superleak (fig. 11*d*). The flow rate gradually decreased with decreasing temperature and down to 1.05°K no indication for superfluid behaviour was found. If ^{3}He has no superfluid properties, it is by no means clear, how the dissolved ^{3}He can join in the superfluid part of the ^{4}He. Furthermore, if one considers the conditions in the various flow experiments, it appears that the ^{3}He always has the same direction as the normal fluid flow. Before we continue, however, we may remark that in the experiments mentioned above (fig. 11*a*, *b*, *c*, *d*), the superleak is always nearly completely filled with liquid, independent of whether the superleak is in direct contact with bulk liquid or with film and saturated vapour. This has been suggested earlier by several authors but it was very convincingly concluded from an extensive study on this subject with pure ^{4}He by Hammel and Schuch (1958) [19]).

Starting with this knowledge the results of the experiment of Hammel and Schuch with the 3.9% mixture, can also be explained if it is assumed that the ^{3}He forms part of the normal fluid which moves to the upper vessel under the influence of the pressure head across the superleak, due to the vapour pressure difference and the difference in surface tension at the two interfaces of the liquid in the superleak. The leak is not completely filled with liquid in this case; for a small part of the length at the low pressure side gas flow takes place. As long as the partial pressure of the ^{4}He in the upper vessel is lower than the partial vapour pressure of the ^{4}He below, the superfluid flow in the liquid is in the same direction as the normal fluid flow. But after this pressure has been reached the net transfer of ^{4}He must be zero, except for the small quantity of ^{4}He, involved in the gradual saturation of the film in the upper vessel and the small change of the composition of the liquid in the lower vessel. The normal part of the ^{4}He in the leak, however, still moves to the upper vessel and must return, therefore, as superfluid. Now the direction of the superfluid flow is opposite to the direction of the normal fluid flow. The normal fluid flow obeys Poiseuille's law, of course, but the ^{3}He must evaporate at the place of the liquid vapour interface somewhere in the slit. The flow phenomena in the superleak are even more complicated now, but one can imagine that the flow rate of ^{3}He

is restricted by the rate of evaporation, yielding a possible explanation for the independence of the ^{3}He flow rate on the gas pressure head across the superleak.

In the experiment of Daunt, Probst, Johnston, Aldrich and Nier the temperature in the Dewar vessel is raised. The vapour pressure inside the vessel is therefore higher than outside and the normal fluid flow will be directed to the outside. But starting with an empty vessel the conditions in the first stage of the experiment are completely similar to the conditions in the experiment of Hammel and Schuch. In the beginning, therefore, ^{3}He must flow into the vessel. When liquid has been collected in the vessel and its temperature is raised, the flow of ^{3}He is in the opposite direction, but the transfer is much smaller now, because the solution inside the vessel is highly diluted. The presence of a small quantity of ^{3}He in the Dewar may be explained in this way.

In the experiment of Wansink and Taconis the conditions are similar to the conditions in the experiment of Daunt *e.a.* after the warm vessel contains some liquid. The normal fluid flow is towards the vessel containing the mixture and, as is known from measurements on the heat conductivity of mixtures the ^{3}He is swept along to the cold end. In the steady state the concentration gradient is almost completely at the end of the leak and the velocity of the ^{3}He is zero. If in this experiment the pure ^{4}He is condensed at first and then the mixture, from the beginning flow of ^{3}He through the slit can be avoided. Indeed during the experiment no ^{3}He in the upper vessel was observed. In all isothermal flow experiments with a bulk liquid mixture at the entrance of the superleak and with a hydrostatic pressure acting on the liquid in the superleak (fig. 11*d*) it has been found that small quantities of ^{3}He flowed through the leak. (Daunt, Probst, Johnston, 1947 [20]; Abraham, Weinstock, Osborne, 1949 [21]; Atkins, Lovejoy, 1954 [22]; Wansink, Taconis, 1957 [7])). In this case normal fluid flow and superfluid flow are in the same direction. Thus there is no reason to believe that the ^{3}He joins in the superfluid, the more so as the velocity of the ^{3}He has always been found small compared with the superfluid velocity. Finally the observed flow phenomena in the film experiment of Esel'son *e.a.* [3]) indicate that in this case the ^{3}He is transferred through the gas phase rather than through the film. Therefore, real experimental evidence for superfluid flow of ^{3}He up to now has not been shown.

The flow rates as observed by Wansink and Taconis with a 1.3% mixture do not agree with our result, as was already mentioned. 1) These flow rates are much smaller than they should be according to our results. 2) The flow rate was found to be slightly dependent on pressure head and this, also, is not confirmed in our experiment. Now we believe that the results of Wansink and Taconis have been influenced by slit effects.

This may be made clear by the following. Wansink and Taconis ascertain that the transfer capacity of the superleak for superflow is larger than the observed flow rate. As a check one can calculate the superfluid velocity in the superleak, assuming the normal fluid velocity to be negligibly small. Starting from the largest observed transfer rate and inserting the superfluid density corresponding to the highest temperature in the slit, the maximum superfluid velocities are found to vary from about 6 cm/s at the lowest bath temperature of 1.5°K to about 1.5 cm/s at a bath temperature of 2.0°K. These velocities are well below the critical velocity which, at 1.5°K is assumed to be of the order of 10–20 cm/s for a slit width of 3.10^{-5} cm. (Once again we remark that the slit contains nearly no ^{3}He).

If the superfluid velocity is indeed below the critical velocity, the flow may be described by the eqs. (7) and (8). Introducing the effective pressure $P_{\text{eff}} = P_{\text{osm}} + P_{\text{f}}$ and following the procedure used in deriving eqs. (11) and (12) we now arrive at the equations:

$$\Delta P = \Delta P_{\text{eff}}. \tag{18}$$

$$\Delta P = C \eta_{\text{n}} \bar{v}_{\text{n}} \tag{19}$$

Eq. (18) implies that the effective pressure head must balance the mechanical pressure head arising from the hydrostatic pressure difference, the vapour pressure difference and the surface tension of the liquid vapour interface at the lower end of the superleak. The maximum contribution from surface tension, however, is of the order of 200–300 cm helium, if one of the radii of curvature of the interface is equal to half the slit width. Since the effective pressure head, corrected for vapour pressure difference and hydrostatic pressure head, varied up to about 1000 cm helium during the measurements, the situation seems incompatible with the assumption that a drop of liquid is present around the gold wires near the entrance of the slit. Most likely the interface is inside the slit and the temperature at the interface is different from bath temperature in such a way that eq. (18) is satisfied for the liquid in the slit. The flow phenomena in the slit may become again more complicated since the slit is only partially filled with liquid in that case. We believe therefore, that the large pressure heads, as calculated by Wansink and Taconis, do not correspond to the real pressure heads. Furthermore we may remark, that quite large temperature differences across the slit must be applied in order to exceed the osmotic pressure of the mixture in the lower vessel. The temperature difference gives rise to a heat leak through the superleak. If the heat conductivity of the superleak is assumed to be completely governed by the two gold wires, the resulting heat leak turns out to vary from 50 to 300 erg/s in the considered range ot effective pressure head, when the lower vessel contains a 1.3% mixture. Because the superleak is surrounded by a vacuum jacket, the heat will be carried off for a great deal by evaporation of liquid near the entrance of the slit.

The observed flow rate is some 10^{-6} cm^3/s and the heat of evaporation 30 erg per 10^{-6} cm^3. Thus the heat leak may also influence the flow rate seriously. We think that the observed low transfer rate and the dependence of transfer rate on pressure head originate from these extra phenomena in the superleak.

Similar difficulties as we mentioned above arise of course when the apparatus of Daunt *e.a.* is used to study the film flow. The experiment of Hammel and Schuch can not be used to study film flow either. With later experiments of the same authors in a similar apparatus, it has been shown that in this experiment the flow through the slit is completely governed by the conditions in and near the exit of the superleak. The flow rate appeared to be independent of whether the entrance of the superleak was immersed in the liquid or not. Therefore, the method employed in our experiment still seems to be most appropriate for measuring the film flow rate of mixtures.

REFERENCES

1) Jackson, L. C. and Grimes, L. G., Phil. Mag. Suppl. **7** (1958) 435.
Atkins, K. R., Liquid Helium, Cambridge University Press 1959, p. 205.
2) Inghram, M. C., Long, E. and Meyer, L., Phys. Rev. **97** (1955) 1453.
3) Esel'son, B. N., Lasarew, B. G. and Lifshitz, I. M., Zh. eksper. teor. Fiz. **20** (1950) 748.
4) Esel'son, B. N., Shvets, A. D. and Bablidze, R. A., Zh. eksper. teor. Fiz. **34** (1958) 233; Soviet Phys. J.E.T.P. **7** (1958) 161.
5) Daunt, J. G., Probst, R. E., Johnston, H. L., Aldrich, L. T. and Nier, A. O., Phys. Rev. **72** (1947) 502.
6) Hammel, E. F. and Schuch, A. F., Phys. Rev. **87** (1952) 154.
7) Wansink, D. H. N. and Taconis, K. W., Commun. Kamerlingh Onnes Lab., Leiden No. 306*b*; Physica **23** (1957) 273.
8) Smith, B. and Boorse, H. A., Phys. Rev. **99** (1955) 328, 346, 358, 367.
9) Kerr, E. C., Proc. fifth internat. Conf. on Low Temp. Phys. and Chem., Madison 1957 (Published in Low Temp. Phys. and Chem., editor J. R. Dillinger, University of Wisconsin Press, Madison 1958, p. 158).
10) Roberts, T. R. and Sydoriak, S. G., Phys. Rev. **118** (1960) 901.
11) Berezniak, N. G. and Esel'son, B. N., Zh. exper. teor. Fiz. **31** (1956) 902; Soviet Phys. J.E.T.P. **4** (1957) 766.
12) Dash, J. G. and Taylor, R. D., Phys. Rev. **107** (1957) 1228.
13) Ham, A. C. and Jackson, L. C., Proc. roy. Soc. **A240** (1957) 243; ref. 1).
14) Ch. III; Matsuda, H. and Van den Meijdenberg, C. J. N., Commun. Suppl. No. 117*d*; Physica **26** (1960) 939; ref. 1).
15) Introduction; Van den Meijdenberg, C. J. N., Taconis, K. W., Beenakker, J. J. M. and Wansink, D.H.N., Commun. No. 295*c*; Physica **20** (1954) 157.
16) Mazur, P., thesis Utrecht, 1951.
17) De Bruyn Ouboter, R., Beenakker, J. J. M. and Taconis, K. W., Commun. Suppl. No. 116*c*; Physica **25** (1959) 1162.
18) Staas, F. A., Taconis, K. W. and Fokkens, K., Commun. No. 323*a*; Physica **26** (1960) 669.
19) Hammel, E. F. and Schuch, A. F., Report LA-2183, Los Alamos Scientific Laboratory of the University of California, Los Alamos.
20) Daunt, J. G., Probst, R. E. and Johnston, H. L., J. Chem. Phys. **15** (1947) 759.
21) Abraham, B. M., Weinstock, B. and Osborne, D. W., Phys. Rev. **76** (1949) 864.
22) Atkins, K. R. and Lovejoy, D. R., Canad. J. Phys. **32** (1954) 702.

CHAPTER III

COMMENTS ON THE THEORY OF THE STATIC HELIUM FILM

Synopsis

Some discrepancies in the theories of the static helium film are discussed. Both Atkins' and Franchetti's theories are criticized. Considering again the effects of Van der Waals forces and acoustical zero point energy, a new derivation is given of formulae for the equilibrium film profile and the density in the film near 0°K. The formula for the profile can be fitted to the experimental results of Ham and Jackson.

1. *Introduction.* As is well known, when a vertical wall is in contact with liquid He II a thick film of He is formed on the wall [1]). Frenkel and Schiff [2]) have put forward theories in which the formation of the film is attributed to the Van der Waals forces between the helium atoms and the substrate. The equilibrium thickness d at a height H above the surface of the bulk liquid is then given by the formula:

$$H = (A/d)^3 \tag{1}$$

where A is a constant which depends slightly on the substrate and is of the order of $2 - 6 \times 10^{-6}$ c.g.s. units.

At first Bijl, De Boer and Michels [3]) pointed out that the zero point energy may be important in determining the film thickness. Assuming that the film liquid may be treated as an ideal Bose-Einstein gas they showed that the equilibrium thickness of the film is given by the formula:

$$H = (B/d)^2 \tag{2}$$

with $B \simeq 10^{-5}$ c.g.s. units.

In this treatment the forces of attraction to the wall have been ignored. As a result the film should be metastable. Moreover, as Mott [4]) has pointed out, the ground state wave function assumed in the theory gives a peculiar variation of density from a maximum at the centre to zero at the wall and at the surface. These consequences indicate that the model should be refined.

Atkins [5]) extended these ideas and put forward a theory in which both

the Van der Waals energy and the zero point energy of the atoms in the film are considered. He calculated the zero point energy due to the longitudinal Debye modes in the film liquid and derived for the zero point energy per unit mass of a slab of thickness d:

$$Z(d, \rho) = Z(\infty, \rho)\left[1 - \tfrac{1}{6}\frac{\lambda_c}{d} + \tfrac{1}{3\,2}\left(\frac{\lambda_c}{d}\right)^2 + \ldots\right] \tag{3}$$

where ρ is the density of the film liquid and λ_c the Debye cut-off wave length of the normal modes. Taking into account the effect of the difference between the density in the film and the density in the bulk liquid he obtained the following expressions for the mean density in the film $\bar{\rho}$ and the equilibrium thickness d:

$$\frac{\bar{\rho} - \rho_0}{\rho_0} = \tfrac{1}{6}\rho_0 K Z_0\left(1 + \frac{\rho}{c}\frac{\partial c}{\partial \rho}\right)\frac{\lambda_c}{d} \tag{4}$$

and

$$H = \left(\frac{A}{d}\right)^3 + \left(\frac{\lambda_c}{d}\right)^2 \frac{Z_0}{g}\left[\tfrac{1}{3\,2} - \tfrac{1}{7\,2}\rho_0 K Z_0\left(1 + \frac{\rho}{c}\frac{\partial c}{\partial \rho}\right)^2\right] \tag{5}$$

where ρ_0 is the density, K the compressibility, $Z_0 = Z(\infty, \rho_0)$ the zero point energy per unit mass and c the velocity of first sound in the bulk liquid; g the gravity constant and A the constant as defined in formula (1).

Ham and Jackson [6]) tried to describe their experimental results on film thickness with a formula of the form:

$$H = (A/d)^3 + (B/d)^2 \tag{6}$$

as was suggested by eq. (5). In the restricted range of height $H = 0.8 - 1.6$ cm and at a temperature 1.3°K they found: $A \simeq 2 \times 10^{-6}$ and $B \simeq 2.5 \times 10^{-6}$.

Substitution of numerical values in eq. (5), however, reveals — as $Z \simeq 1.6 \times 10^8$ erg/g, $K \simeq 1.2 \times 10^{-8}$ cm²/dyne, $\rho_0 = 0.145$ g/cm³ and $(\rho/c)\,(\partial c/\partial \rho) \simeq 2.8$ — that the coefficient of $1/d^2$ should be negative, in disagreement with the experimental data.

Although Franchetti [7]) noted an error in eq. (3) and pointed out that the sign of the second term on the right hand side should be positive, this correction leads only to a change of sign in eq. (4) but eq. (5) remains unaltered. The change of sign in eq. (4), however, would indicate that the mean density in the film is lower than the bulk liquid density, contrary to Atkins' expectation.

Franchetti derived a formula like eq. (6) taking into account the effect of temperature. He neglected, however, the effect of the difference between the density in the film and the density of the bulk liquid, which is important

in Atkins' formula. Moreover, Franchetti's calculation leads to:

$$Z(d, \rho) = Z(\infty, \rho)\left[1 + \tfrac{1}{72}\left(\frac{\lambda_c}{d}\right)^2 + \ldots\ldots\right] \qquad (7)$$

which is different from formula (3).

Recently Dzyaloshinskiĭ, Lifshitz and Pitaevskiĭ [8]) developed a theory in which the Van der Waals energy of the film is related to the dielectric properties of the system wall-film-vapour (vacuum). They argue that this contribution to the energy leads essentially to a film profile as given by formula (1) but that the value of the constant A as calculated by Schiff cannot be trusted at all.

Considering the energy of acoustical origin they criticize Atkins' method of determining the cut-off frequency, asserting that the cut-off should be made as in the calculation of the zero point energy in vacuum surrounded by metal as was done by Casimir [9]). This cut-off frequency is independent of the size of the vacuum and it is completely determined by the metal. The contribution of acoustical origin calculated with this cut-off appears to be negligibly small, but leads in principle also to a film profile of the form (1). However, contrary to Casimir's case, in the problem of acoustical zero point energy the cut-off should be more strongly correlated with the degrees of freedom in the film liquid itself, than with the properties of the system surrounding the film*). Thus Atkins' method of determining the cut-off seems more appropriate in this case than Casimir's method and we still think it worthwhile to consider in detail the energy of acoustical origin as well the energy of electromagnetic origin.

2. *The film at* 0°K. In obtaining the expression for film profile and density in the film the important quantity is the change of free energy of the system of He atoms per unit mass when they are brought from the bulk liquid onto the wall. As in this section we restrict ourselves to 0°K, the free energy is equal to the energy of the system. The change of the energy density will, in general, depend on the height above the surface of the bulk liquid, the distance from the wall, the thickness of the film, the density, *etc.* Of course, it is very difficult to determine the change of energy density from first principles of quantum mechanics, so we have to make some assumptions or use some models in constructing this expression. Once this expression is set up, we can obtain the expression for the total energy change due to the formation of the film on the wall and the remaining work is only to minimize this total energy change by varying both density and thickness of the film, in order to obtain the expressions for film profile and density in the film.

*) The same argument has been put forward by Franchetti [14])

3. *The uniform model.* The calculation has been performed by Atkins [5]) assuming uniform density in the film; but already two points in this calculation require closer consideration:

I) the expression for the zero point energy; eqs. (3) and (7).

II) the influence of the Van der Waals forces on the mean density and hence on the film profile.

Consider a square film slab of side L and thickness d. A typical Debye wave of frequency ν and velocity c has direction cosines l_x, l_y, l_z given by:

$$\frac{n_x c}{2 l_x \nu} = L \qquad \frac{n_y c}{2 l_y \nu} = L \qquad \frac{n_z c}{2 l_z \nu} = d \tag{8}$$

n_x, n_y, n_z being integers. Because the maximum value of n_z is relatively small in this case it is important whether $n_z = 0$ should be included or excluded in computing the total zero point energy. Including $n_z = 0$ corresponds to the assumption that the vibration may have antinodes at the surface of the film; while excluding $n_z = 0$ corresponds to the assumption that the vibration must have nodes at the surface of the film. In this connection we note the following: (1) The zero point energy of atoms arises via Heisenberg's uncertainty principle from the confinement of the atoms in some restricted range. (2) In contrast to elastic solid, in liquid He II only longitudinal waves can be assumed to exist as elastic waves. No elastic force can oppose the transverse motion of the atoms. This typical situation can be seen in a linear chain of atoms in which only longitudinal elastic forces exist. In a transverse direction atoms can move freely, yielding no zero point energy. Therefore, unless we can suitably take into account the potential energy loss due to the density change near the surface of the film caused by penetration of the wave function through the interface, we must strictly confine the atoms to the box with sides L, L and d. This means that we should exclude $n_z = 0$. When this correction is made, the calculation, similar to Atkins' calculation leads to

$$Z(d, \rho) = Z(\infty, \rho) \left[1 + \tfrac{1}{6} \frac{\lambda_c}{d} + \tfrac{1}{32} \left(\frac{\lambda_c}{d} \right)^2 + \ldots\ldots \right] \tag{9}$$

instead of eq. (3).

Franchetti [7]) derived eq. (7) starting from the idea that the change of zero point energy is due to the change of the boundary of the Debye distribution of representative points in wave vector space and he showed that the small deviations from the spherical boundary introduced by replacing integration by summation lead to a change of the zero point energy proportional to $(\lambda_c/d)^2$ when the density of representative points in wave vector space is kept constant. In fact, the mean density of representative points in wave vector space decreases when $n_z = 0$ is excluded and Franchetti's statement that the first order term should vanish ceases to be true when this change of density is included. For this reason, the

geometrical argument of Franchetti to explain the difference between the coefficients of $(\lambda_c/d)^2$ in eqs. (3) and (7) is also not quite correct and there remains no reason to prefer Franchetti's choice of boundary to the choice of Atkins. Further calculations, therefore, are based on the validity of eq. (9).

II) In Atkins' model it is assumed that the density in the film is uniform at a fixed height, *i.e.*, the density is assumed to be independent of the distance from the wall. The notion of mean density of the whole film however is not very significant. As already pointed out by Atkins and Franchetti the density near the wall is very high and there will be a solid layer with thickness 5–10 Å, depending on the substrate. The thickness of this layer will be almost independent of d, because close to the wall the Van der Waals energy is dominant. It seems therefore more significant to consider the liquid part only when the assumption of uniform density is made.

Accordingly, the lower limit (r) of the integral in the expression for the total energy is equal to the thickness of the solid layer (table I). The nearly constant energy of the solid layer is irrelevant in our problem and is therefore omitted in the expressions for ΔE.

The contribution of the change of internal energy to the total energy density has been represented by $\Delta U = \{(\rho - \rho_0)/\rho_0\}^2/2\rho_0 K$ where ρ_0 is the density and K the compressibility of the bulk liquid.

The influence of surface tension has been considered separately. Only that part of surface tension is included which is concerned with the Van der Waals forces between the He atoms and not the "dynamical" part due to surface waves. The appropriate term in the expression for the energy density is $\alpha_2/(a + d + r_0 - z)^3$ where r_0 is some length of the order of an interatomic distance in liquid helium.

The expressions for the mean density and the film profile are tabulated in table I; the corresponding numerical results in table II. We may remark that the terms due to the Van der Waals energy are large enough to change the sign of the coefficient of f^2 in the expression for gH. In the expression for the mean density these terms nearly compensate the effect of increased zero point energy. The resulting mean density differs very slightly from ρ_0.

4. *Non-uniform model.* Although the uniform model gains some significance by restricting the consideration to the liquid part of the film, it still has some shortcomings. The distance r of the solid liquid interface from the wall can not be determined within this model and r is a parameter on which $\bar{\rho}$ and gH depend rather strongly. Thus it is desirable to have a model in which r can be determined. Moreover, near the wall the density in the film will be higher than at the surface of the film, because near the wall the gain of Van der Waals energy through increase of density is predominant, while near the surface the gain of zero point energy through reduction of density

TABLE I

$\varepsilon_1(z) = gH - \frac{\alpha_1}{z^3} + \frac{\alpha_2}{(r+d+r_0-z)^3}$ $\varepsilon_2(d,\rho) = \frac{1}{2\rho_0 K}\left(\frac{\rho-\rho_0}{\rho_0}\right)^2 + Z(d,\rho) - Z(\infty,\rho)$ $\varepsilon(z,d,\rho) = \varepsilon_1(z) + \varepsilon_2(d,\rho)$	$Z(\infty,\rho) = Z_0\left\{1+\omega\frac{\rho-\rho_0}{\rho_0}\right\}$ $\omega = {}^1/_3 + \frac{\rho}{c}\frac{\partial c}{\partial \rho}$ Assumption: $\frac{\partial\omega}{\partial\rho} = 0$	$Z(d,\rho) = Z(\infty,\rho)\{1+\sigma(d,\rho)\}$ $\sigma(d,\rho) = f/6 + f^2/32 + \ldots$ $f = \frac{\lambda_c}{d} \qquad \lambda_c \sim \rho^{-1/3}$
Notation: $Q = Z_0(\omega + {}^2/_3)/6$	$P = -Z_0/32 + \rho_0 K Q^2/2$	$R = \frac{\alpha_1}{r^2\lambda_c} - \frac{\alpha_2}{r_0^2\lambda_c}$
Atkins $\Delta E = \tilde{\rho}\int_{r_0}^{d}\varepsilon(z,d,\tilde{\rho})\,dz$	$\frac{\tilde{\rho}-\rho_0}{\rho_0} = -\rho_0 K Q f_0$	$gH = \frac{\alpha_1}{d^3} - P f_0^2$
Uniform model $\Delta E = \tilde{\rho}\int_{r}^{r+d}\varepsilon(z,d,\tilde{\rho})\,dz$ $= \tilde{\rho}\{\tilde{\varepsilon}_1 + \varepsilon_2(d,\tilde{\rho})\}$	$\frac{\tilde{\rho}-\rho_0}{\rho_0} = -\rho_0 K\{Qf + \tilde{\varepsilon}_1\}$ $= -\rho_0 K\{Q - \frac{1}{2}R\}f_0$	$gH = \frac{\alpha_1-\alpha_2}{(r+d)^3} +$ $+ f_0^2[-P + \frac{1}{2}\rho_0 K R\{Q - \frac{1}{4}R\}]$
Non-uniform model $\Delta E = \int_{r}^{r+d}\rho(z)\,\varepsilon(z,d,\rho)\,dz$	$\frac{\rho(z)-\rho_0}{\rho_0} = -\rho_0 K\{Qf + \varepsilon_1(z)\}$ $\frac{\tilde{\rho}-\rho_0}{\rho_0} = -\rho_0 K\{Q - \frac{1}{2}R\}f_0$	$gH = \frac{\alpha_1-\alpha_2}{(r+d)^3} +$ $+f_0^2\left[-P + \frac{1}{2}\rho_0 K Q\left\{R + 1.2\rho_0 K\left(\frac{\alpha_1^2}{r^5\lambda_c} - \frac{\alpha_2^2}{r_0^5\lambda_c}\right)\right\}\right]$
Non-uniform model; constant compressibility $\varepsilon_2(d,\rho) = \frac{1}{\rho_0 K}\left[1 - \frac{\rho_0}{\rho} - \frac{\rho_0}{\rho}\log\frac{\rho}{\rho_0}\right] +$ $+ Z(d,\rho) - Z(\infty,\rho)$	$\frac{\rho(z)-\rho_0}{\rho_0} = -\frac{\rho_0 K\{Qf + \varepsilon_1(z)\}}{1 + \rho_0 K\{(3Q - \frac{1}{2}Z_0)f + \varepsilon_1(z)\}}$ $\frac{\tilde{\rho}-\rho_0}{\rho_0} = -\{\rho_0 K Q - \frac{1}{2}\varphi_1\}f_0$	$gH = \frac{\alpha_1-\alpha_2}{(r+d)^3} +$ $+ f_0^2\,[-P + {}^1/_9\,(Q + \frac{1}{2}Z_0)\varphi_1 + \frac{1}{2}\,Q\varphi_2]$

Note: φ_1 and φ_2 are simple functions of r and r_0, which are not given explicitly here. The numerical values are of the order of unity.

TABLE II

	$10^{14}\alpha_1$ erg cm^{3}g^{-1}	r Å	10^6A cm$^{4/3}$	10^6B cm$^{3/2}$	10^6C cm$^{4/3}$	$\frac{\tilde{\rho}-\rho_0}{\rho_0}$
Atkins $H=\left(\frac{A}{d}\right)^3-\left(\frac{B}{d}\right)^2$	[1]) 7.6	—	4.2[5]	3.5	—	$-0.17f$
	6.2	—	4.0	3.5	—	$-0.17f$
	2.4	—	2.9	3.5	—	$-0.17f$
Uniform model $H=\left(\frac{A}{d}\right)^3+\left(\frac{B}{d}\right)^2$	[1])[2]) 7.6	[3]) 8.0	4.2[5]	4.0	—	$+0.01f$
	6.2	—	4.0	—	—	—
	2.4	6.0	2.9	3.4	—	$-0.07f$
Uniform model incl. surface tension	[1])[4]) 7.6	[3]) 8.0	4.2	4.0	—	$-0.02f$
	6.2	—	3.9[5]	—	—	—
	2.4	6.0	2.8	2.6	—	$-0.10f$
Non-uniform model $H=\left(\frac{A}{d}\right)^3+\left(\frac{B}{d}\right)^2$	[1])[2]) 7.6	8.2[5]	4.2[5]	7.7	—	-0.00^5f
	6.2	7.8	4.0	7.3	—	$-0.02f$
	2.4	5.6	2.9	6.1	—	$-0.06f$
	[5]) 0.7° Exp.	3.7	1.9	4.6	—	$-0.09f$
Non-uniform model incl. surface tension	[1])[4]) 7.6	8.2[5]	4.2	7.2	—	$-0.03f$
	6.2	7.8	3.9[5]	6.7	—	$-0.05f$
	2.4	5.6	2.8	5.3[5]	—	$-0.08f$
	[5]) 0.9[3] Exp.	4.1	1.9	3.9[5]	—	$-0.12f$
Non-uniform model constant compressibility $H=\left(\frac{A}{d}\right)^3+\left(\frac{B}{d}\right)^2-\left(\frac{C}{d}\right)^3$	[1])[2]) 7.6	9.4	4.2[5]	6.8	0.82	$-0.03f$
	6.2	8.8	4.0	6.5	0.79	$-0.04f$
	2.4	6.4	2.9	5.2	0.65	$-0.08f$
	[5]) 0.7° Exp.	4.2[5]	1.9	3.7	0.44	$-0.11f$
Non-uniform model incl. surface tension constant compressibility	[1])[4]) 7.6	9.4	4.2	6.0	0.77	$-0.06f$
	6.2	8.8	3.9[5]	5.7	0.73	$-0.07f$
	2.4	6.4	2.8	4.1	0.57	$-0.10f$
	[5]) 0.9[3] Exp.	4.7	1.9	2.6	0.32	$-0.13f$
Experiment of Ham and Jackson			1.9	2.5		

Notes table II

[1]) It is not possible to derive a value for α from the theory of Dzyaloshinskiĭ *e.a.* because our knowledge about the dielectric properties of helium is incomplete. We therefore based our calculation on the constants as obtained from "potential theory". According to this theory the expression α_1/z^3 indicates the difference between the Van der Waals potential of the wall and the Van der Waals potential of a "wall" of He atoms with bulk liquid density; thus $\alpha_1 = \alpha_{wall} - \alpha_{He}$. In order to see the effect on the final results we used various values of α_{wall} as calculated by Schiff and Franchetti ($\alpha_{Cu} = 7.8 \times 10^{-14}$; $\alpha_{glass} = 6.4 \times 10^{-14}$; $\alpha_{Barium\ stearate} = 2.6 \times 10^{-14}$ erg cm^3 g^{-1}) Franchetti calculated α_{He} based on atomic data: $\alpha_{He} = 0.26 \times 10^{-14}$ erg cm^{3}g^{-1}. Some information can also be obtained from the data on surface tension. The effective part of surface tension originating from Van der Waals forces may be written as $\gamma_e = \alpha_{He}/2r_0^2$, where r_0 is some length of the order of an interatomic distance in the liquid. Substituting $r_0 = 3.6$ Å and $\gamma_e = 0.13$ erg cm^{-2} according to Atkins' theory [10]) on surface tension, we find: $\alpha_{He} = 0.23 \times \times 10^{-14}$ erg cm^{3}g^{-1}.

[2]) The effect of surface tension can be excluded by substituting $\alpha_2 = 0$ in the expressions in table I.

[3]) Values of r according to the calculation by Franchetti [7])

[4]) We used $\alpha_2 = \alpha_{He} = 0.23 \times 10^{-14}$ erg cm^{3}g^{-1} (see note 1)

[5]) α_1 and r are calculated, using Ham and Jackson's experimental value of A. From r and α_1 we deduced B.

is predominant. Therefore the inclusion of the non-uniformity of density may influence the results significantly.

For these reasons we tried to set up a model in which the density depends on the distance from the wall. The expression for the total energy change in this case is more or less analogous to that in the uniform model (see table I). We have no proof that the expression for the contribution of zero point energy is right in the case of non-uniform density, but the extension

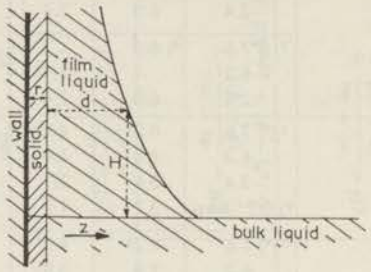

Fig. 1

we made here seems rather natural. Moreover, the formulae finally obtained show that the effect of zero point energy is not changed principally with this assumption. The condition that ΔE is minimum with respect to $\rho(z)$ now leads to (we assumed $\partial\omega/\partial\rho = 0$):

$$\tfrac{3}{2}\left(\frac{\rho-\rho_0}{\rho_0}\right)^2+[1+\tfrac{5}{18}\rho_0 K Z_0\omega f]\frac{\rho-\rho_0}{\rho_0}+\rho_0 K\,[\varepsilon_1(z)+\tfrac{1}{6}Z_0(\omega+\tfrac{2}{3})f]=0. \quad (10)$$

As we are concerned with thick films $\frac{5}{18}\rho_0 K Z_0\omega f \simeq \frac{1}{4}f \ll 1$ and provided $6\rho_0 K\,|\varepsilon_1(z)| \ll 1$ or $z > 10$Å, eq. 10 gives:

$$\frac{\rho(z)-\rho_0}{\rho_0} = -\rho_0 K[\varepsilon_1(z)+\tfrac{1}{6}Z_0(\omega+\tfrac{2}{3})f]. \quad (11)$$

Because $|\varepsilon_1(r+d)| \ll \frac{1}{6}\rho_0 K Z_0(\omega+\frac{2}{3})f$ the density at the surface of the film is now given by:

$$\frac{\rho(r+d)-\rho_0}{\rho_0} = -\tfrac{1}{6}\rho_0 K Z_0(\omega+\tfrac{2}{3})f. \quad (12)$$

Substituting $\rho(r)$ equal to the solidification density of liquid helium we obtain the value of r from eq. (10). Without making a serious error the validity of eq. (11) may be extended to $r < z < 10$Å. Integration of eq. (11) now yields the expression for the mean density, the result being the same as in the uniform model. From eqs. (10) and (11) and the equation obtained by minimizing ΔE with respect to d we find the expression for the film profile as given in table I. The numerical results are tabulated in table II.

In order to investigate whether the assumption we made with respect

to the internal energy is very critical for the final results, we also made a calculation based on another assumption, namely a liquid of constant compressibility. In this case it is also possible to calculate the contribution of one higher order term in f, assuming $\partial\omega/\partial\rho = 0$ (C in table II). These results are also given in the tables. We may remark that the value of B in this model calculated from the experimental value of A, including the effect of surface tension, is comparable to Ham and Jackson's experimental value of B at 1.3°K. The influence of higher order terms seems negligibly small.

5. *Effect of finite temperature.* Below 1°K the energy excitation in liquid helium is mainly due to phonons. Moreover, according to Landau and Khalatnikov [10]), the mean free path of a phonon is larger than 10^5 Å below 1°K. This implies that the size effect directly influences the energy of the phonon system. Therefore, so long as we discuss the properties of a film several hundred angströms thick below 1°K we may use the same model simply replacing the energy by the free energy.

We can use Franchetti's expression for the free energy of Debye phonons excluding the zero point contribution. As a result we find that the effect of finite temperature in the expression for film profile and density in the film is very small; smaller than 1% below 1°K. Therefore below 1°K the formulae of table I are valid. We have only to insert the appropriate values for the physical quantities in these equations at the temperature under consideration.

6. *Discussion.* Unfortunately up to the present there are no experimental data on the film thickness below 1°K, where the theory can be valid. In this temperature region only data on the flow of the film exist, which seem to indicate an increase of transfer rate below 0.9°K. But whether this is due to an increase in thickness can not be decided at this moment.

In table II we see that the values of A and B obtained from the values of α as calculated by Schiff or Franchetti are higher than Ham and Jackson's experimental values. In view of the remark of Dzyaloshinskiĭ, Lifshitz and Pitaevskiĭ that the existing calculations of α cannot be trusted, we tentatively determined the value of α from the experimental value of A measured by Ham and Jackson at 1.3°K. The value of B thus obtained is in better agreement with the experimental value of B, especially when the effect of surface tension is included. In the beginning we thought that the special models should give very different values of B, because the effect of zero point energy is of the second order in f, the first order term being cancelled. The many numerical results given in table II, however, show that the values of B agree in order of magnitude in the different models. Recently Anderson, Liebenberg and Dillinger [12]) reported measure-

ments on the film profile at 1.4°K up to a height of 40 cm. The value of B deduced from their results is much smaller than the value of A, which leads to the conclusion that the results agree better with formula (1) than with formula (6). As may be seen from table II we performed calculations starting from various values of A; in none of these cases did the corresponding value of B appear to be insignificantly small.

Another remarkable result is that all models for the mean density of the film liquid yield values either a little smaller or almost equal to the density of the bulk liquid. This is contrary to Atkins' result based on eq. (3) for the zero point energy; and it shows that the blowing-up effect of the zero point energy is large enough to more than compensate for the squeezing effect of the Van der Waals forces in the thick film. It suggests also that Atkins' interpretation of the data on differential entropy as obtained by Strauss [13]) should be reconsidered. It is not only dangerous to apply the formula for the density in the film to the case of very thin films, but the definition of differential entropy should also be made more precise when, indeed, a size effect exists.

REFERENCES

1) For the general survey of He films see, for instance,
   a) Atkins, K. R., Liquid Helium, Ch. 7 (Cambridge Univ. Press, Cambridge, 1959).
   b) Atkins, K. R., Progress in Low Temperature Physics, Vol. II, Ch. 4 (North-Holland Publ. Co., Amsterdam, 1957).
2) Schiff, L. I., Phys. Rev. **59** (1941) 838.
   Frenkel, J., J. Phys. Moscow **2** (1940) 345.
3) Bijl, A., De Boer, A. and Michels, J., Physica **8** (1941) 655.
4) Mott, N. F., Phil. Mag. **40** (1949) 61.
5) Atkins, K. R., Canad. J. Phys. **32** (1954) 347; Conférence de Physique des Basses Températures (Paris, 1955) p. 100; Ref. 1), *a*) p. 227.
6) Ham, A. C. and Jackson, L. C., Proc. roy. Soc. A **240** (1957) 243.
7) Franchetti, S., Nuovo Cimento **4** (1956) 1504; **5** (1957) 183.
8) Dzyaloshinskiĭ, I. E., Lifshitz, E. M. and Pitaevskiĭ, L. P., Zh. eksper. teor. Fiz.(U.S.S.R.) **37** (1959) 229; Soviet Physics J.E.T.P. **37** (1960) 161.
9) Casimir, H. B. G., Proc. K. Ned. Akad. Wetensch. (Amsterdam) **51** (1948) 793.
10) Atkins, K. R., Can. J. Phys. **31** (1953) 1165.
11) Landau, L. D. and Khalatnikov, I. M., Zh. eksper. teor. Fiz. (U.S.S.R.) **19** (1949) 637, 709.
12) Anderson, O. T., Liebenberg, D. H. and Dillinger, J. R., Phys. Rev. **117** (1960) 39.
13) Strauss, A. J., Ref. 1), *b*) p. 114.
14) Franchetti, S., Nuovo Cimento **16** (1960) 1158.

Acknowledgements. I wish to express my sincere thanks to Mr. F. A. Staas, Mr. K. Fokkens and Mr. J. A. van Gelderen for their help during the measurements and to the members of the technical staff of the laboratory, especially Mr. H. Kuipers, Mr. A. Ouwerkerk, Mr. H. Nater and Mr. L. Neuteboom for their able assistence.

I am indebted to Mr. C. Knobler for correcting the English text.

SAMMENVATTING

In dit proefschrift worden enige onderzoekingen beschreven over het fonteineffect en de heliumfilm, verschijnselen die optreden in vloeibaar helium beneden de λ-temperatuur.

De experimenten zijn uitgevoerd met behulp van toestellen welke in hoofdzaak bestaan uit twee vaten verbonden door een z.g. superlek dat dient als semipermeabele wand, doorlaatbaar voor de superfluide component en nagenoeg ondoorlaatbaar voor de normale component van Helium II. Het superlek bestaat in de meeste gevallen uit een roestvrij stalen buisje, gevuld met samengeperst Parijs'rood poeder.

Bij het eerste experiment, dat in de inleiding wordt besproken, bevindt zich aanvankelijk in beide vaten een kleine hoeveelheid Helium II. Door het aanbrengen van een temperatuurverschil tussen beide vaten stroomt de vloeistof via de film uit het koude naar het warme vat. De resterende fonteindruk over het superlek oefent zijn invloed uit op de film die nog aanwezig is op de wanden van het koude vat. Dit komt tot uitdrukking in een daling van de druk van het gas dat in evenwicht is met de film. Uit de gemeten drukafname wordt afgeleid dat de fonteindruk in overeenstemming is met de formule van H. London.

Hoofdstuk I is gewijd aan het fonteineffect in Helium II onder druk. Bij dit experiment zijn beide vaten gevuld met vloeibaar helium terwijl de druk is verhoogd tot boven de verzadigde dampspanning. Uit directe metingen van het fonteineffect in het temperatuurgebied van 1.15°K tot 2.00°K, bij drukken variërend tussen de verzadigde dampspanning en 25 atm., is de entropie als functie van temperatuur en druk berekend, uitgaande van de formule van H. London. Een goede aansluiting is gevonden aan de entropiewaarden bij de verzadigde dampspanning, berekend uit de soortelijke warmte metingen van Kramers, Wasscher en Gorter. Met behulp van deze en andere gegevens is een entropie diagram samengesteld voor het temperatuurgebied tussen 1.15°K en de λ-lijn. In het laatste gedeelte van dit hoofdstuk zijn berekeningen van de parameters van het rotonen spectrum vermeld. De resultaten worden vergeleken met die van directe metingen van het excitatie spectrum d.m.v. neutronenverstrooiing.

In hoofdstuk II komt het transport door de film, in evenwicht met vloeibare mengsels van ^{3}He en ^{4}He, ter sprake. In dit geval bevinden zich in beide vaten mengsels van ^{3}He en ^{4}He van verschillende concentraties. De vloeistof stroomt onder invloed van de osmotische druk, via de film, van het ene naar het andere vat. Uit de metingen blijkt dat de transportsnelheid onafhankelijk van de drijvende kracht, doch afhankelijk van de temperatuur, de ^{3}He concentratie en de hoogte van de film boven het vloeistofoppervlak is. In dit hoofdstuk worden verder enige critische beschouwingen gewijd aan de verschijnselen die optreden bij stroming van Helium II door nauwe spleten.

Hoofdstuk III bevat een overzicht van de bestaande theorieën over de statische heliumfilm. Uitgaande van verschillende modellen worden uitdrukkingen afgeleid voor de dikte van de film als functie van de hoogte en voor de dichtheid van de film. De formule voor het filmprofiel is in overeenstemming met de experimentele gegevens van Ham en Jackson maar niet met die van Anderson, Liebenberg en Dillinger. De berekende gemiddelde dichtheid van de filmvloeistof blijkt kleiner of bijna gelijk aan de dichtheid van bulk vloeistof te zijn.